RESEARCH ON DIGITAL TRANSDUCER PRINCIPLES

Volume VII

DIELECTRIC PROPERTIES OF THIN POLYMER FILMS

ELECTRONIC MATERIALS RESEARCH LABORATORY

THE UNIVERSITY OF TEXAS

COLLEGE OF ENGINEERING

AUSTIN

RESEARCH ON DIGITAL TRANSDUCER PRINCIPLES

Volume VII

DIELECTRIC PROPERTIES OF THIN POLYMER FILMS

for the

NATIONAL AERONAUTICS AND SPACE ADMINISTRATION

GRANT NGR-44-012-043

Covering the Period

July 1, 1967 - June 30, 1968

by

Yen Shan Chuang

William H. Hartwig

The University of Texas at Austin

Austin, Texas 78712

Page intentionally left blank

PREFACE

Previous work on Metal-Polymer-Silicon thin film structures has been reported as a part of the search for digital transducer concepts. The existence of a break in the current - voltage characteristic of this device when reverse-biased has been regarded as a basis of digital action. If it could be studied in sufficient detail to understand and control the phenomena, the application to integrated silicon microelectronic circuits would be attractive. The device is not nearly as simple as might be assumed by its simple structure. The V-I characteristic is influenced in many ways, some very subtle, and it need only be pointed out that surface states in the semiconductor play a vital role. The state of knowledge of surface physics of semiconductors is far from adequate, but very intensive work is being done by many groups in the semiconductor industry. The success of the MIS Digital Transducer is by no means assured, but the possibility of success makes the effort worthwhile.

The task of resolving the various physical phenomena has been made easier by this separate study of the charge transport processes and energy storage processes in the polymer film alone. Previous work by the group served as a starting point and greater detail was revealed by improvements in the method of fabrication and measurement of behavior. This work will be compared to the work reported on in Volume VIII in future reports.

ABSTRACT

Thin films of polymerized DC-704 oil, ranging in thickness from 50 Å to 1000 Å, can be formed by electron beam bombardment with reasonable good reliability and compatibility. The characterizing properties are strongly dependent on the method of preparation and invironmental conditions. There are a number of processes which can provide dielectric relaxation behavior. The actual mechanisms are extremely difficult to identify and thus phenomenological expressions have been derived.

Experiments were conducted on metal-polymer-metal structures to investigate the characteristics. The structures consisted of aluminum electrodes with the polymer film between them.

It is found that there are two dielectric relaxations in the film, a high frequency dispersion with a low frequency dispersion superimposed. The relaxation time is estimated to be between 1.9 and 4.5×10^{-7} seconds for the high frequency dispersion. The low frequency peak occurs well below 100 Hz. The relative dielectric constant at 1 K Hz is 2.8 and the index of fraction is 1.39.

The experimental capacitance-time curves show a decrease in capacitance with aging for every specimen. On further analysis it becomes clear that the percentage decrease in capacitance is a bulk function rather than a surface function and is attributable to the absorption of oxygen.

A very high dielectric strength, routinely being higher than 10^6 volt/cm. is observed. The strength decreases when the energy of formation increases. The dependence of capacitance on temperature and dc bias is seen. Non-linear dc conductivity of the polymer film is observed, and the data

appears to be consistent with more than one charge transport mechanism. Temperature dependence of capacitance is consistent with Debye relaxation and Maxwell-Wagner interfacial polarization.

TABLE OF CONTENTS

	Page
PREFACE	iii
ABSTRACT	iv
LIST OF FIGURES	viii
I. INTRODUCTION	1
A. Electron Beam-Induced Polymer Films	1
B. Previous Work	2
C. Chemical Structure of Polymer Films	4
D. Objects of Present Work	5
II. DIELECTRIC LOSS MECHANISM	7
A. Introduction	7
B. Debye Theory	8
C. Maxwell-Wagner Effects	13
D. Dielectric Loss Due to Conductivity	17
E. Cole and Cole Plot	18
III. EXPERIMENTAL PROCEDURE	22
A. Introduction	22
B. The Metal-Insulator-Metal Structure	22
1. MIM Capacitor Configurations	22
2. Substrate	22
3. Metal Electrodes	24
4. Polymer Insulator	25

Page

C. Fabrication Apparatus 26

1. Vacuum System 26

2. Electron Gun 27

D. Measurement Equipment 29

1. Capacitance Bridge 29

2. Constant Temperature Chamber 30

3. Resistance Bridge 31

IV. EXPERIMENTAL RESULTS 32

A. Introduction 32

B. Film Growth 32

C. A.C. Measurement 33

1. Dielectric Constant 33

2. Dielectric Relaxation 35

3. Modified Cole and Cole Plot 38

4. Aging Effects 47

5. Temperature Dependence 54

6. Effects of voltage on Capacitance 54

D. D.C. Dielectric Strength 58

E. Electrical Conductivity 59

V. SUMMARY OF CONCLUSION AND RECOMMENDATION 62

A. Conclusion 62

B. Recommendation for Further Research 63

BIBLIOGRAPHY 64

VITA 67

LIST OF FIGURES

Number		Page
1	Debye Curve	12
2	Complex plane Loci of the complex dielectric constant and equivalent circuits	21
3	MIM structures	23
4	Cathode Ray Tube and its control circuits	28
5	Resistance Bridge	31
6	Film growth	34
7	Capacitance vs. frequency for samples of different thickness	36
8	Dissipation factor vs. frequency for samples of different thickness	37
9	Capacitance vs. frequency for sample No. 18	39
10	Dissipation factor vs. frequency for Sample No. 18	40
11	ε'' vs. frequency and ε' vs. frequency for Sample No. 18	41
12	Loss factor vs. dielectric constant for Sample No. 18	42
13	Two dissipation regions for polymer film	44
14	Capacitance vs. time for samples of different thickness at 1K Hz	48
15	Per cent decreases of capacitance vs. time for samples of different thickness at 1K Hz	49
16	Resultant percentage capacitance changes vs. thickness at 1K Hz	50
17	Dissipation factor vs. time for Samples of different thickness	52
18	Inverse capacitance vs. temperature	55
19	Dielectric constant vs. frequency and loss factor vs. frequency for Sample No. 48	56
20	Loss factor vs. dielectric constant at different temperature for Sample No. 48	57
21	V-I charactertistics	61

CHAPTER I

INTRODUCTION

A. Electron Beam-Induced Polymer Films

It has been known for many years that exposure of organic vapors in the atmosphere of vacuum system to an electron stream results in formation of an organic polymer film. The mechanism was attributed to a free radical polymerization of the organic vapor[1,2]. This technique of polymerization became an attractive one. Following a suggestion by Buck and Shoulder[3] that these polymer films might be useful for electrical insulation in thin film circuits, several workers have reported the properties of polymer dielectric films formed by electron bombardment of silicone vapor molecules.

Polymer dielectric film prepared in this way have some advantageous features over those formed by other process. Since they are formed by a surface reaction, they can be formed selectively, i.e., only where the electron beam struck the surfaces; lines down to 1 micron wide have been "drawn". If the vapor is chemisorbed on the solid surface (such as DC-704 oil) an extremely thin dielectric film may be formed, down to one or two molecular thickness. Practically, these polymer films have very low incidence of pinholes down to 50 Å thick. The absence of large intrinsic stress in these films reduces the likelihood of cracking or rupture after deposition and was proposed for insulator between metal films in Cryotrons (Super-Conductor Memory Stores).

Investigations have showed[9] that the dielectric properties of polymer films are extremely dependent on the deposition procedure and substance used. A considerable wide range of these properties is accessible because of the large

number of polymerizable species available. Polymer film may offer unusual properties over and above thos pertaining to electrical insulation. With sufficient understanding of the physical and chemical process, it should be possible to fabricate polymer films with specific properties for specific devices, such as the digital transducer.

The polymer dielectric films have great promise both electrically and structurally for both room temperature and cryogenic microcircuitry. It does not seem, however, at this stage that these techniques have been applied fully. There is still much to be studies.

B. Previous Work

The formation of polymerized films on the surfaces of apparatus by electron bombardment of residual gases such as pump oil was first observed accidently in electron microscopy. Ennos[1] and Poole[2] attributed the mechanism to free radical polymerization of pump oil fragments. After this phenomenon was proposed for preparing insulation for circuit fabrication by Buck and Shoulders, systemtical investigation have been performed.

A preliminary study of polymerization of DC-704 pump oil was reported by Christy[6] in 1960, with the substrate at 25°C, a current density of 0.4 mA/cm^2 and an accelerating voltage of 225V be obtained a maximum growth rate of 18Å/min, the films resistivity of 10^4 Ω cm and breakdown strength of 10^7 v/cm. The secondary electron emission from polymer surface during bombardment was first observed by Holland and Laurenson[11], Mann[5] investigated a dependence of growth rate on secondary electron emission for DC-704 oil.

The work on DC-704 oil was subsequently extended by Christy[6] and Mann[5] to include properties of the polymer dielectric films. Both of them observed non-ohmic conductivity at large applied voltages and the change with time of the dielectric properties of the films. The dielectric constant before aging was 2.8 ± 0.3 with dissipation factor between 0.5 and 1.5 at 1 KHz, and the capacitive changes occurred after growth depending on environment. Holland and Laurenson[9] investigated the electric properties of polymerized DC-704 films as a function of electron energy, bombardment time, substrate temperature and presence of other gases. They found that polymerized DC-704 films grown at the low rate of 4 Å/min and at impingement ratio (silicone molecules to electrons) of 1 : 3 and 1 : 42 had dielectric constant of 2.6 and 4.0 and a dissipation factor at 1 KHz of 0.003 and 0.015 respectively. Thus reducing the molecular to electron flux ratio raises the dielectric constant and dissipation factor. Raising the pressure of the residual gas to 3×10^{-4} torr with oxygen during polymer growth reduced the film resistivity, whereas raising the hydrogen pressure increased the resistivity.

Hill[8,15] conducted a detailed investigation of the properties of polymerized dimethylpolysiloxane and DC-704 oil, he found that polymer films of DC-704 oil degraded and poor insulators when formed at electron beam energies of 750 eV. For the energy range used (50-300 eV) the growth rate was a function of the substrate potential. A maximum growth rate of 48 Å/min occurred at 120 V which was much higher than that reported by Holland and Laurenson[9] at substrate potential 0.4 to 2 KV.

A recent investigation[19] of polymerized DC-704 films have showed the frequency dependence of the capacitance at rather low frequencies. Such a dependence is completely unexpected in common dielectrics.

Other materials have been polymerized by electron bombardment, including butadiene[13], styrene[14], methyl methacrylate[15], epoxy resin, triphenylsilanol[17,18] and other more complex molecules.

In general, the polymer films have a wide variation in dielectric properties, depend on the method of preparation, and changes occurred after growth in air.

C. Chemical Structure of Polymer Films

The silicone compound used for growing polymer films in this study is DC-704 pump oil, even though the specific arrangement of methyl and phenyl groups are not known, the chemical structure of DC-704 is of the following form:

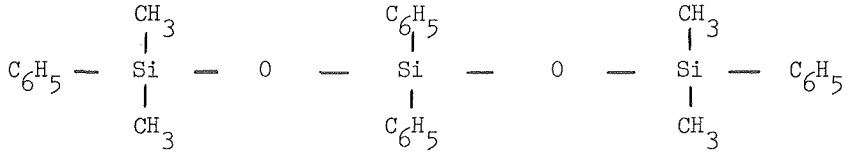

When silicone molecules are exposed to electron bombardment, the bond most likely to fracture and promote cross-linking are those of methyl terminals. The cross-linking is of either following kind:

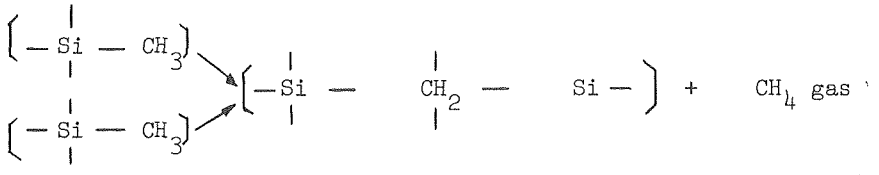

methylene cross-link

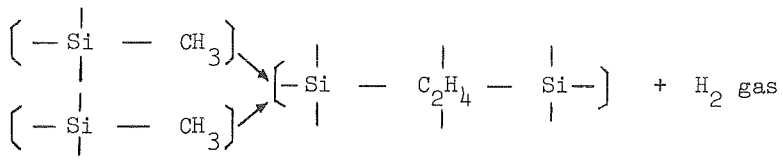

ethlene cross-link

As a result of the electron irradiation process, cross-links are formed at randon throughout the polymer.

Cross-linking is often proportional to the radiation dose and higher degrees of cross-linking occuring at random produce a heterogeneous materials which is partly insoluble and partly soluble. This distinction arises purely from the statistical distribution of the links which, if sufficiently close may give rise to the formation of closed networks. The soluble fraction of the polymer decreases with increasing degree of cross linking.

The cross-linking of the polymer can be inferred from the direct evidence, that the polymer does not soften and flow upon heating and from the fact that the polymer does not dissolve in solvents such as acetone. The actual degree of cross-linking has not been determined.

D. Objectives of Present Work

The summary which has been presented appears to indicate several points for investigation.

1. Using metal-polymer-metal structure, find whether dielectric properties of polymerized DC-704 films are predictable and to establish the conditions which are necessary for consistent results. Mention has already been made of the dependence of properties on preparing procedure by many workers.

2. Due to the lack of specific information on the nature of chemical structure of the polymer films, it will be more practicable to find a phenomenological model for the observed dielectric relaxation.

3. To investigate the long term changes in dielectric constant and dissipation factor by keeping the devices in different environment and compare with previous works.

4. To perform other related experiments and make suggestions for further research.

CHAPTER II

DIELECTRIC LOSS MECHANISM

A. Introduction

The vast majority of polymers have structures containing dipoles and, as in the case of monomeric liquids and glasses, they exhibit dielectric dispersion superposed on atomic and electronic polarization. In the simplest cases the behavior is very much like that of polar liquids in that a dispersion region and loss maximum are observed and can be described by a most-probable relaxation time and a distribution parameter. Usually polymers exhibit anomalous despersion and dielectric loss at frequencies many decades lower than simple compounds and thus correspond to a broad distribution in relaxation times[20]. The situation is further complicated by conductance due to impurities or multiple dispersion regions that are generally attributed to multiple phases or modes of dipole rotation. Therefore the interpretation of the dielectric behavior of polymers is still incomplete[21].

There are non-polar polymer, i.e., structures in which there are no permanent dipole moments, which generally show fairly low dielectric constants, practically no dielectric loss, and slight frequency dependence of either of these quantities. The polarization which such non-polar material exhibits is principally due to distortions of electronic and atomic structures. Dielectric losses in Polyethylene[22] and Paraffin[23] have been reported and were attributed to impurities, oxidation and end-groups.

The polymer films which are formed by electron bombardment, can be expected to have concentration of free radicals. These free radicals perhaps

can act as electron traps and have effect of increasing the electron transport through the film. Oxygen or water vapor trapped during deposition can account for an ionic conductivity in the films. The existance of a d.c. ionic conductivity mechanism gives rise in an a.c. experiment to low frequency losses[24]. If the films are non-homogeneous the migration of electrons or ions which diffused into the polymer films produces interfacial polarization.

Mann[5] has judged the polymerized DC-704 films to be non-polar based on the observation of small change in dielectric constant between 4 and 300^{0}K. But in this experimental study, all the polymerized DC-704 films indicated dielectric dispersion, and the dielectric losses are much higher than what expected for non-polar material. The data from ellipsometer measurements also indicated that the index of refraction of the polymer films is 1.39 corresponding to a dielectric constant of 2.8 at 1 KHz. This evidence shows that Mann's judgement is hard to be agreed with in this case.

However, here are a large number of process which can provide dielectric relaxation behavior and the actual mechanism are extremely difficult to identify. The Debye type phenomenological equations might fit the data if contributions from several polarization process are added to account for the broad band of relaxation times.[25] In the present study, attempts will be made to work out a model for the observed dielectric behavior following the lines of the classical theory of Debye, without knowing the actual mechanism.

B. Debye Theory

The classical theory of the effect for polar liquids is due to Debye[26]. Under the influence of an alternating electric field a system of polar molecules

is supposed to diffuse by rotary Brownian motion toward an equilibrium distribution in molecular orientation, corresponding to a resultant dielectric polarization. If the frequency of the applied field is sufficiently high rotatory diffusion becomes to slow for the establishment of equilibrium with the field. As a result the polarization acquires a component out of phase with the field. The displacement current also acquires a conductance compenent in phase with the field resulting in thermal dissipation of energy from the field. The dependence of the loss factor on frequency is determined by the relaxation time, which is the interval required for the polarization in a static field to diminish to a fraction of e^{-1} of its equilibrium value when the field is suddenly removed.

A convenient development of the Debye equations by Böttcher[38] is shown below.

Let ε_s be the static dielectric constant and ε^∞ be the dielectric constant at very high frequency. The polarization may assumed to be made up of two parts, P_1 and P_2, P_1 keeps in phase with the applied field and P_2 is established more slowly and lags behind E.

Since

$$D = \varepsilon^* \varepsilon_o E = \varepsilon_o E + P \qquad (1)$$

$$P_1 = (\varepsilon^\infty - 1)\varepsilon_o E \qquad (2)$$

where ε_o = dielectric constant of vacuum.

For static conditions

$$P = (\varepsilon_s - 1)\varepsilon_o E \qquad (3)$$

When a field, $E = E_o e^{j\omega t}$ is applied suddenly, P_2 approaches its final values at rate proportional to the difference remaining

$$\frac{dP_2}{dt} = \frac{1}{\tau} \left[(\varepsilon_s - \varepsilon^\infty)\varepsilon_o E_o e^{j\omega t} - P_2\right] \tag{4}$$

The general solution of this equation is

$$P_2 = ce^{-t/\tau} + \frac{(\varepsilon_s - \varepsilon^\infty)}{1 + j\omega t} \varepsilon_o E_o e^{j\omega t} \tag{5}$$

The first term on the right hand side will decrease to an infinitely samll value after some time and therefore it may be negelected. Thus we obtain for the total polarization

$$P = P_1 + P_2 = \left[(\varepsilon^\infty - 1) + \frac{\varepsilon_s - \varepsilon^\infty}{1 + j\omega t}\right]\varepsilon_o E_o e^{j\omega t} \tag{6}$$

From this formula, we see that P is a sinusoidal function of the time with the same frequency as the applied field. The complex part between the square brackets shows that it is retarded in phase with respect to E.

$$D = \varepsilon^* \varepsilon_o E_o e^{j\omega t} = \left[1 + (\varepsilon^\infty - 1) + \frac{\varepsilon_s - \varepsilon^\infty}{1 + j\omega t}\right]\varepsilon_o E_o e^{j\omega t} \tag{7}$$

Thus the complex dielectric constant ε^* is given by

$$\varepsilon^* = \varepsilon' - j\varepsilon'' \tag{8}$$

$$= \varepsilon^\infty + \frac{\varepsilon_s - \varepsilon^\infty}{1 + j\omega t}$$

which can be written

$$\varepsilon' = \varepsilon^{\infty} + \frac{\varepsilon_s - \varepsilon^{\infty}}{1 + \omega^2\tau^2} \tag{9}$$

$$\varepsilon'' = \frac{(\varepsilon_s - \varepsilon^{\infty})\,\omega\tau}{1 + \omega^2\tau^2} \tag{10}$$

where ω = the angular frequency,

τ = the relaxation time

Examination of Eq (10) shows that ε'' approaches zero both for samll and for large values $\omega\tau$, which it is a maximum for

$$\omega\tau = 1 \tag{11}$$

For this values of $\omega\tau$, Equs (9) and (10) give

$$\varepsilon'_{max} = \frac{\varepsilon_s + \varepsilon^{\infty}}{2} \tag{12}$$

$$\varepsilon''_{max} = \frac{\varepsilon_s - \varepsilon^{\infty}}{2} \tag{13}$$

Typical curve of this type is shown in Figure-1 and the dissipation factor is given by

$$\tan\delta = \frac{(\varepsilon_s - \varepsilon^{\infty})\omega\tau}{\varepsilon_s + \omega^2\tau^2\varepsilon^{\infty}} \tag{14}$$

with a value at the maximum of

$$\tan\delta_{max} = \frac{\varepsilon_s - \varepsilon^{\infty}}{2(\varepsilon_s\,\varepsilon^{\infty})^{1/2}} \tag{15}$$

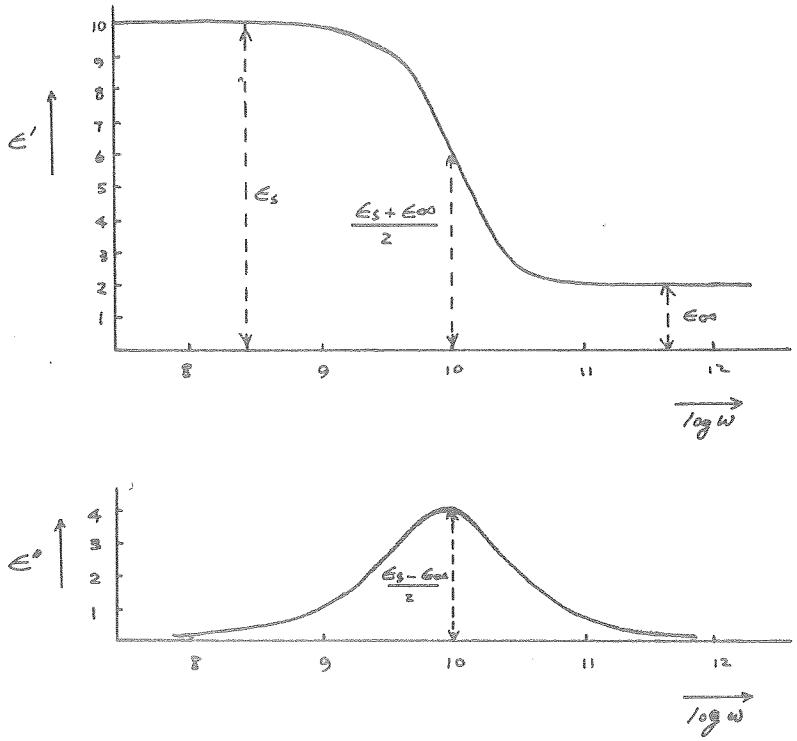

FIG - 1. Debye Curves

In this treatment, the relaxation time is for the macroscopic relaxation process, and is different from the microscopic or molecular relaxation time which Debye used in the original derivation.

Fröhlich[28] has given an analysis of the distribution of relaxation times. If $y(\tau)d\tau$ is the contribution to static dielectric constant of the group of dipoles having individual relaxation times in a range near the total contribution of all the dipoles is

$$\varepsilon_s - \varepsilon^\infty = \int_0^\infty y(\tau)d\tau \tag{16}$$

and Eqs. (9) and (10) becomes

$$\varepsilon' = \varepsilon^\infty + \int_0^\infty \frac{y(\tau)d\tau}{1 + \omega^2\tau^2} \tag{17}$$

$$\varepsilon'' = \int_0^\infty \frac{y(\tau)\omega\tau d\tau}{1 + \omega^2\tau^2} \tag{18}$$

The values for ε'' evidentally consist of a superposition of Debye curves $\omega\tau/(1 + \omega^2\tau^2)$, with different positions and heights of their respective maxima, and thus give the lower, broader curves.

C. Maxwell-Wagner Effect (Interfacial Polarization)

Besides molecular orientation, migration of ions or electrons can produce energy losses in dielectrics. When the dielectric is homogeneous this produces conductivity losses which decrease in magnitude with increasing frequency

(see 11 D). In a non-homogeneous material without a conducting path between the electrodes the final current must always be zero. A type of polarization is produced by the charged particles which move through the conducting regions and accumulate on the surface separating the conducting regions.

Attempts were made by Maxwell[29] to treat the simplest model where the dielectric is in two phases parallel to the electrodes, one of which is conducting and the other is non-conducting. He showed that the behavior was in accordance with the Debye equations. Wagner[30] treated the case where the spherical particles of phase 1 having a real dielectric constant ε'_1 and a conductivity σ_1 are sparsely distributed through phase 2, which was a real dielectric constant ε'_2 and a negligibly small conductivity provided that the fraction p of the phase 1 in relation to the total volume of dielectric is small, the apparent dielectric constant observed for the material as a whole is then found to be

$$\varepsilon^* = \varepsilon^\infty + \frac{\varepsilon_s - \varepsilon^\infty}{1 + j\omega t'} \tag{19}$$

which can be written

$$\varepsilon' = \varepsilon^\infty + \frac{\varepsilon_s - \varepsilon^\infty}{1 + \omega\tau'^2} \tag{20}$$

$$\varepsilon'' = \frac{(\varepsilon_s - \varepsilon^\infty)\omega\tau'}{1 + \omega^2\tau'^2} \tag{21}$$

with

$$\varepsilon_s = \varepsilon_2' (1 + 3p) \tag{22}$$

$$\varepsilon^\infty = \varepsilon_2'[1 + \frac{3p(\varepsilon_1' - \varepsilon_2')}{\varepsilon_1' + 2\varepsilon_2'} \tag{23}$$

$$\varepsilon_s - \varepsilon^\infty = \frac{9p\varepsilon_2'^2}{\varepsilon_1' + 2\varepsilon_2'} \tag{24}$$

$$T' = \frac{(\varepsilon_1' - 2\varepsilon_2')\varepsilon_o}{\sigma_1 \times 10^2} \tag{25}$$

Obviously, Eqs (19), (20), and (21) are identical to Eqs (8), (9) and (10).

From these equations, we can obtain from the frequency of maximum absorption, for σ_1 in ohm^{-1} cm^{-1}

$$f_{max} = 1.8 \times 10^{12} \sigma_1/(\varepsilon_1' + 2\varepsilon_2') \tag{26}$$

with a corresponding value of ε at the maximum given by

$$\varepsilon''_{max} = \frac{\varepsilon'}{2} [\, 1 + \frac{3p\ (\varepsilon_1' - \varepsilon_2')}{(\varepsilon_1' + 2\varepsilon_2')} \,] \tag{27}$$

As long as each of the materials in itself is homogeneous there is only one relaxation time which depends only on the properties of the two materials, when the properties of individual spheres are different, it leads to a distribution of relaxation times.

This treatment has been extended to consider the case where the dispersed particles are no longer sphrical but may be regarded as orolate or oblate ellipsoids. The following general conclusions may be stated[36].

1. The loss factor ε'' increases linearly with the volume fraction of the dispersed phase but τ' is independent of this fraction.

2. ε'' and τ' are both independent of the size of dispersed particles provided they are small compared with the thickness of the specimen.

3. The relaxation time, τ' is inversely proportional to the conductivity of the dispersed phase while the loss factor ε'' is independent of σ. Consequently only particles of low conductivity can cause the frequency of maximum loss to lie within or below the audio frequency range.

4. For frequencies above the absorption frequency, the shape of the particles has little effect on the loss factor ε''.

It is evident that small quantities of impurities may seriously affect the dielectric properties of a material if it leads to the formation of an additional phase. Various aspect of the theory have been confirmed experimentally by Hamon and Meakings[31], using water dispersed in paraffin wax which is crystalline polymer.

A quantitative treatment in any practical case is difficult partly because there is no wholly satisfactory way of specifying or treating mathematically the shapes actually assumed by the conducting impurities which are likely to segregate at grain boundaries and similar places; and partly because the electrical properties of the dispersed material may differ from the properties of the same material in bulk form.

D. Dielectric Loss Due to Conductivity

The relation of the apparent conductivity to dielectric constant and loss is first analyzed by Murphy and Morgan[32]. In an ideal dielectric there would be no free-ion conduction, but, in actual insulating materials, Joule heat may be produced by the drift of electrons or free ions in the applied field. The total heat developed is the sum of the dielectric loss and the Joule heat. The dielectric loss is thus proportional to the measured ac conductivity minus dc conductivity.

If a dielectric material of dielectric constant ε fill the space between the parallel plates of a two plate condenser which has a distance d cm and an alternating potential $V = V_o e^{j\omega t}$ is applied, the current density in the dielectric is then

$$\frac{dq}{dt} = j\omega (\varepsilon' - j\varepsilon'')\varepsilon_o \frac{V_o e^{j\omega t}}{d}$$

$$= (\varepsilon' \omega \varepsilon_o + j\varepsilon' \omega \varepsilon_o) E_o e^{j\omega t}$$

$$= (\sigma' + j\sigma'') E_o e^{j\omega t} \qquad (28)$$

where

$$\sigma' = \varepsilon'' \varepsilon_o \omega \qquad (29a)$$

$$\sigma'' = \varepsilon' \varepsilon_o \omega \qquad (29b)$$

From Eqs (29a)the relation is obtain

$$\varepsilon''_{dc} = \frac{\sigma'}{\omega\varepsilon_o} = \frac{3.6 \times 10^{12}\pi\sigma'}{\omega} \qquad (30)$$

for σ' in ohm^{-1} cm^{-1}

Substituting Eqs (10) in (29a) the effective conductance is given by

$$\sigma' = \frac{(\varepsilon_o - \varepsilon^\infty)\varepsilon_o\omega^2\tau'}{1 + \omega^2\tau'^2} \qquad (31)$$

Mere impurities may have sufficient influence to make necessary the correction of the measured loss factor by subtracting from it the loss factor. This technique has been applied to analyze the treated Neoprene[33] etc. with a satisfactory results.

For a mixed material the loss factor may be regarded as the sum of three distinct effects, that is

$$\varepsilon''(\text{observed}) = \varepsilon''_{dc} + \varepsilon''\ (\textit{Maxwell-Wagner}) + \varepsilon''\ (\text{Debye}) \qquad (32)$$

E. Cole and Cole Plot

It has been mentioned in previous sections that both the expressions for dielectric dispersion due to Debye theory (dipolar polarization) and Maxwell-Wagner effect (interfacial polarization) are identical in form with Eqs (8).

$$\varepsilon^* = \varepsilon^\infty + \frac{\varepsilon_s - \varepsilon^\infty}{1 + j\omega\tau}$$

differing only in the significance of the parameters ε_s, ε^∞ and one might thus expect these relations to have a very general validity as a description of dispersion process.

By modifing Eqs (8), Cole and Cole[34] developed an empirical formula which represents the dispersion process for a considerable number of materials.

$$\varepsilon^* = \varepsilon^\infty + \frac{\varepsilon_s - \varepsilon^\infty}{1 + (j\omega\tau_o)^{1-\alpha}} \tag{33}$$

τ_o = the most probable relaxation time

α = empirical constant with values between 0 and 1, a measure of the distribution of the relaxation times.

The real and imaginary part of the complex dielectric constant, instead of Eqs (9) and (10) are given by

$$\varepsilon' = \varepsilon^\infty + \frac{\varepsilon_s - \varepsilon^\infty}{2}\left\{1 - \frac{\text{Sinh}\,[(1-\alpha)\,X]}{\text{Cosh}\,[(1-\alpha)X] + \text{Sin}\,(\frac{\alpha\pi}{2})}\right\} \tag{34}$$

$$\varepsilon'' = \frac{(\varepsilon_o - \varepsilon^\infty)\,\text{Cos}\,(\frac{\alpha\pi}{2})}{2\left\{\text{Cosh}\,[(1-\alpha)X] + \text{Sin}\,(\frac{\alpha\pi}{2})\right\}} \tag{35}$$

where $X = \ell n\omega\tau o$

When the values of ε'' are plotted as ordinates against those of ε' as abscissas, a semicircular arc is obtained intersecting the abscissa axis at $\varepsilon' = \varepsilon_\infty$ and $\varepsilon' = \varepsilon_s$. The center of the circle of which this arc is a part lies below the abscissa axis, and the diameter of the circle drawn through the center from the intersection at ε_∞ make an angle $\alpha\pi/2$ with the abscissa axis. When α is zero, the diameter lies in the abscissa axis, there is but one relaxation time, and the behavior of the material conforms to the simple Debye theory, the complex plane loci of the complex dielectric constant and equivalent for dielectrical are showed in Fig-2.

When a substance has more than one relaxation mechanism, or when the material is a mixture, the observed loss-frequency curve is the resultant of two or more different curves and, therefore, departs from the simple Debye or Cole and Cole Plot.

If the dielectric substance in question has two regions of dispersion and absorption, an additional parallel branch may be added to the equivalent circuits[35], and the equivalent complex dielectric constant can then be given by

$$\varepsilon^* = \varepsilon_\infty + \frac{K_1}{1 + (j\omega\tau_1)^{1-\alpha_1}} + \frac{K_2}{1 + (j\omega\tau_2)^{1-\alpha_2}} \qquad (38)$$

Where

$$\varepsilon_\infty = \frac{\varepsilon'}{\varepsilon_s}$$

$$K_1 = \frac{\varepsilon_1}{\varepsilon_s}$$

$$K_2 = \frac{\varepsilon_2}{\varepsilon_s}$$

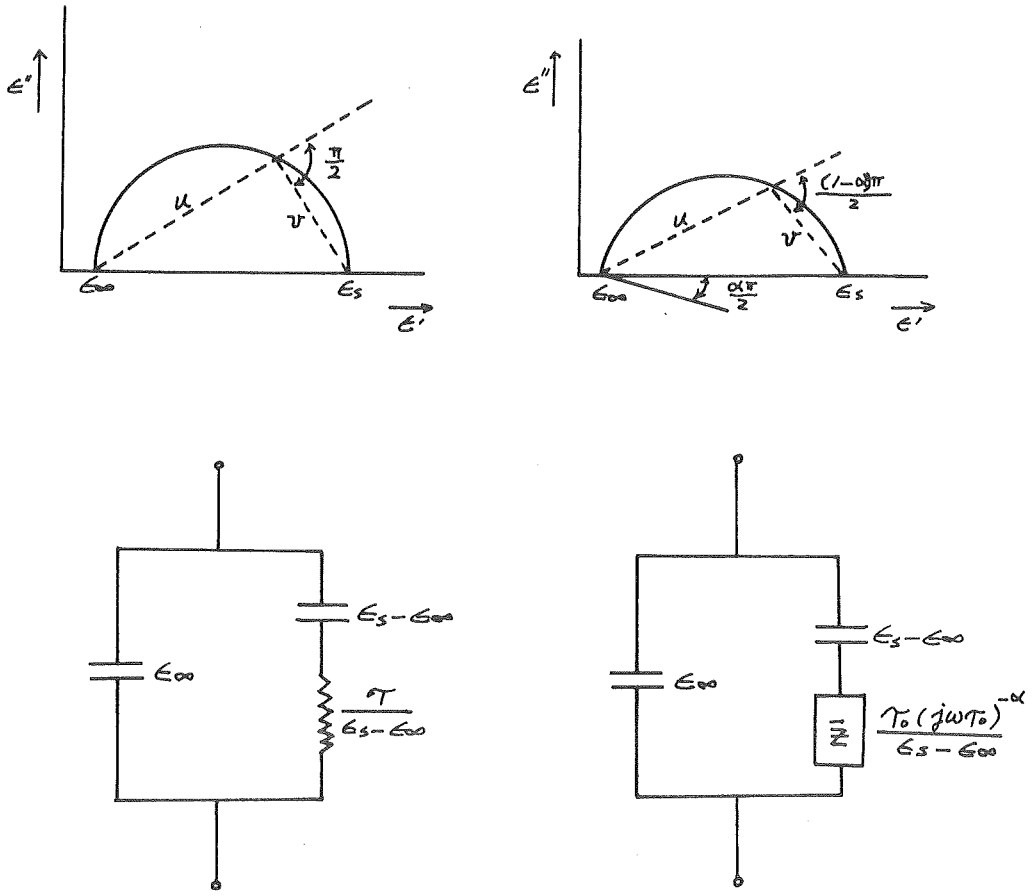

Fig - 2. Theoretical complex plane loci of the complex dielectric constant and equivalent circuits for dielectrics

(a) Debye Theory (b) experimental evidence

CHAPTER III

EXPERIMENTAL PROCEDURE

A. Introduction

The metal-Insulator-Metal structures were in the form of crossed metal strips, 1.1 mm wide, with an insulating layer between them. For all structures the metal electrodes were evaporated aluminum film, and the insulator was polymerized silicone film. Even though the polymerized silicone films were initially reliable (uniform thickness and free from pinholes) in a thickness range to 50 to 300 Å, unprepared microscope slides yielded a large number of film pinholes and improper evaporation of metal electrodes causes creepage beyond the edge of the masked areas of the substrates. Both attributed to short-circuited samples. Well developed technology was required to prepare a sufficient number of samples with good enough precision to test. Much care was taken to minimize the effects of unknown factors.

B. The Metal-Insulator-Metal Structure

1. MIM Capacitor Configuration

Samples were formed by evaporating the base aluminum strip, depositing a polymerized silicone film of desired thickness and then evaporating another aluminum strip on top at right angle to the first aluminum strip, these aluminum strips served as capacitor plates and provided electrical contact for measurement. The physical configuration of the MIM structure was shown in Figure-3.

2. Substrate

The microscope glass slides were used as substrate in all experiments. Early attempts to evaporate capacitors on cleaned, but otherwise

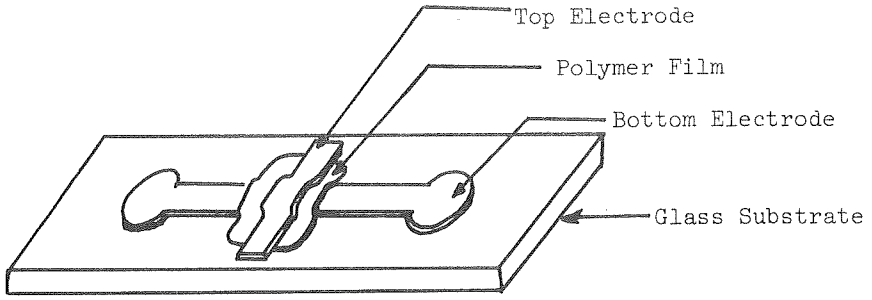

(a)

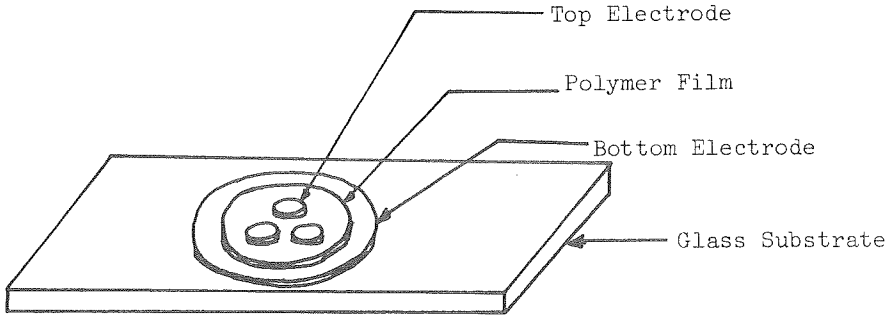

(b)

Fig - 3. MIM structure. (a) Basic structure
(b) Three-one-one structure

unprepared microscope slides yielded a large number of film pinholes, accompanied by electrical shorts between the capacitor plates, Microscopic examination of the glass slides showed extended areas of increased surface roughness with probably represented recrystallization zones. The slightest contaminant film on the slide also caused serious deterioration in uniformity. Therefore all the slides were inspected under a 20X microscope to reject slides with obvious imperfections. Slides were at first immersed in quartz cleaning solution for five minutes and then rinsed by deionized water, finally the vapor from boiling trichloroethylene was used to remove the residue particles and grease adhering to the surface. These procedure were performed immediately before the slides were put into the vacuum system to assure the meticulous cleaness of the substrates.

3. Metal Electrodes

The yield of short-free capacitors was further increased by a proper choice of the metal used for the capacitor electrodes. Metals of high evaporation temperature, such as nickel, resulted in a higher percentage of failures, probably due to penetration of the polymer film by the highly energized metal atoms, silver, an obvious choice because of its low evaporation temperature and high conductivity, also gave poor results. Its high mobility may have caused shorts by grain-boundary diffusion. Aluminum yield the best result. This can probably be explained by its low evaporating temperature combined with a decreased surface mobility caused by the affirmity of aluminum for oxide bond[36] with aluminum electrodes. A yield of more than 80% of short-free capacitors has been obtained. 99.99% pure aluminum was used as the electrode material. The

aluminum was vaporized by a five-turn tungsten heating coil about 20 cm, from the substrate. Two sheet stainless steel masks, each with a single slit 1.1 mm wide, were held within 0.5 mm of the substrate to form the electrode because the masks could not make perfect contact with the substrate. Creepage of the evaporated metal caused the width of the aluminum electrodes to vary from sample to sample. The actual width of the electrodes was determined by using a 10X Zeiss calibrated eye-piece. In all experiments, the area of samples which varied from 1.24 mm^2 to 1.56 mm^2 had been normalized to 1.3 mm for comparison of results.

The thickness of the electrodes were made about 1000 Å. A strip of the deposited aluminum of this thickness 2 cm length and 1.1 mm wide had 9 to 12 ohms dc resistance. It is negligible compared to the capacitor which is in series with it, on the order of 10^8 ohms.

The main disadvantage of aluminum electrode is the dificulty of making electrical contact. They resist even Hg-In as a contact wetting agent. The deposition of aluminum electrodes were performed between 10^{-3} to 10^{-6} torr. Experiments showed that the electrodes deposited in 10^{-3} to 10^{-4} torr had the highest adhesion to the substrate. The electrodes deposited at 10^{-6} torr proved to be easier to melt into the Hg-In wetting agent and caused difficulties in making contact. There appears to be sufficient oxygen present to permit the formation of the intermediate oxide layer at the aluminum-glass interface during deposition of the electrode at a residual air of pressure of 10^{-3} to 10^{-4} torr. The high adhesion is due to the oxide layer at the interface.

4. Polymer Insulator

Polymer thin films deposited by electron bombardment of DC-704 diffusion pump oil vapor were used as insulator. Besides the oil present

in the vacuum system as a result of back-streaming from the diffusion pump, an extra heated oil source was located near the substrate to increase the supply of oil molecules on the substrate available for polymerization. The polymerization activation energy was provided by a 360 V electron beam.

Less than 10 eV of energy is required to cause one cross-link to form[6]. The growing rate of the polymer film is therefore, independent of the electron energy, but strongly dependent on the ratio of electrons to oil molecules reaching the surface of the substrate.

It has been found that not only the pump oil, but also silicone vacuum grease, machined metal surfaces and ordinary grease removers produced organic vapors in the vacuum system which can be converted into solid polymer films by the bombardment of low energy electron beam. For compatibility of the polymer film efforts has been made to prevent organic contamination.

C. Fabricating Apparatus

1. Vacuum System

A NRC vacuum system with an 24" bell jar was used to fabricate the MIM capacitors. Its 8" three-stage diffusion pump, using DC-704 pump oil, yields a vacuum of 5×10^{-5} torr or better in about an hour. The polymer growth was performed in this region. The evaporation of the bottom aluminum electrode was done at 5×10^{-4} torr for stronger adhesion but the top electrode was evaporated at the same pressure as the polymer growth to avoid the possible damage to the already-deposited polymer.

As described by Fitzgibbons[19], the bell jar was equipped with a three-station evaporation apparatus, to permit the fabrication of Metal-Polymer-Metal Capacitor without breaking the vacuum. Two metal deposition stations used glass

evaporation shields to prevent the evaporate from coating the bell jar and other equipment contained within the bell jar. The glass evaporation shields were long enough to keep the substrate, or the already-deposited polymer, away from the tungsten filament to avoid possible damage caused by heat. A set of gimbaled rings hold the Cathode Ray tube (electron beam source) in alignment with the target and were sufficiently sturdy to prevent misalignment during reloading procedures.

An outside driver, working through rubber-sealed feedthrough, provided the mechanism for rotating the sample holder from station to station. A vertical motion in each station places the holder onto a pair of alignment pins to assure accurate positioning.

An extra source of DC-704 oil in a crucible with a surface of 4 cm^2 was heated to 60^{o}C and the temperature was monitored with a copper-contantan thermocouple. The extra oil source was kept at 60^{o}C at least an hour before the polymer film was deposited in an effort to reach equilibrium.

All of the machined parts to be used in the bell jar were cleaned by means of mechanical polish and chemical etch to strip surface contamination, tools were thoroughly cleaned and white gloves were worn whenever operating of the vacuum system. The vacuum system was evacuated when not in use.

2. Electron Gun

A 902A cathode ray tube served as the source of electrons for the polymerization process. The screen and the upper portion of the tube was removed and the tube was held in the grimble mount in the vacuum chamber. Figure 4 shows the external control circuit used to provide for the beam current adjustment, accelerating potential adjustment, the aiming of the electron beam spot on

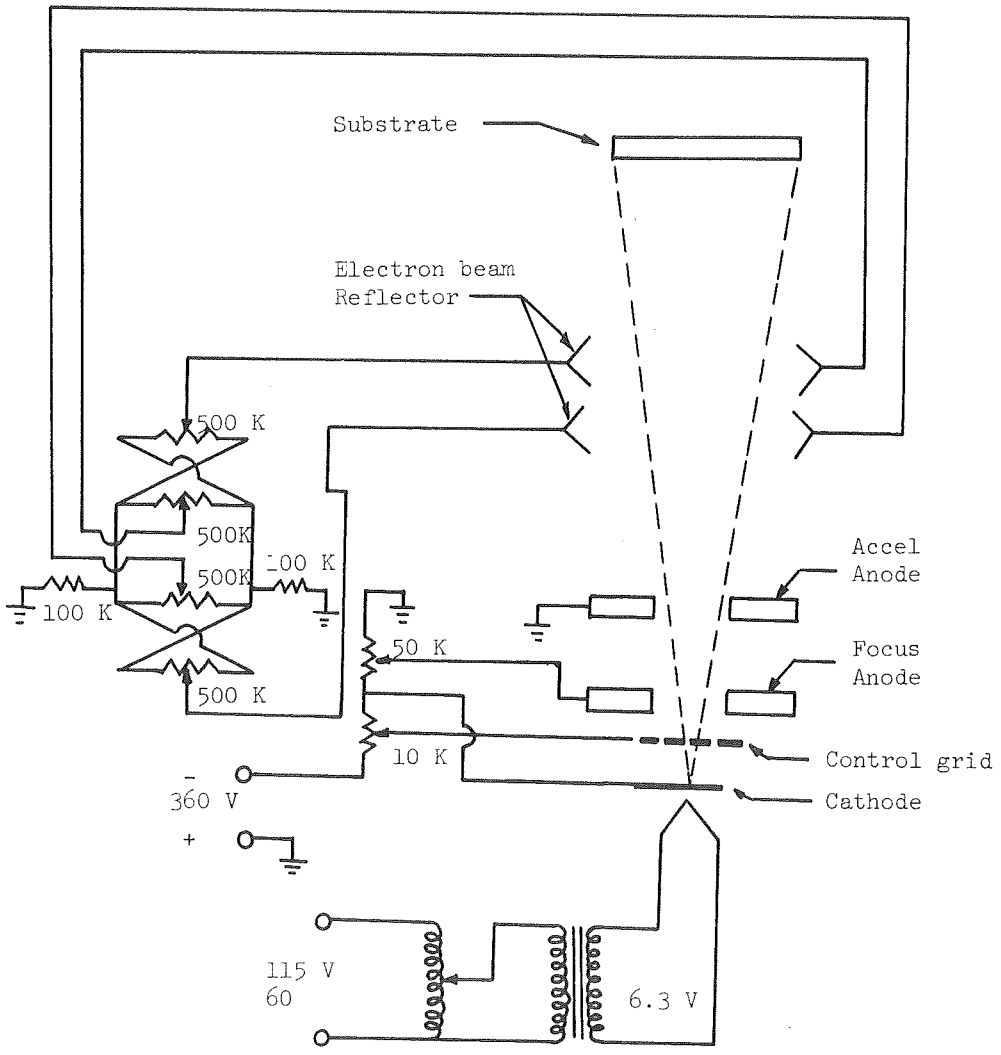

Fig - 4. The cathode ray tube and its control circuit

the substrate, and adjustment of the size of the spot. For greater growing rate, the first anode was grounded and the substrate was biased above the first anode to collect secondary electrons.

To align the electron beam spot, the phosphor screen from the cathode ray tube was placed on the alignment substrate which was at the substrate position. By adjusting the relative position of the spot on the screen and a cross mark on the alignment substrate, the alignment was achieved without difficulty.

If the cathode ray tube filament was turned off the emission of the cathode decreased rapidly, and the electron beam had some nonuniformity in it cross section. The reasonable explanation was that the oil molecules which fell on the cathode surface would burn when the filament was turned on, and the organic residue on the cathode surface reduced its efficiency. This was avoided almost completely by operating the filament at 9V to 10V for about 10 minutes before each run. Keeping the filament operating at 3V to 4V in the vacuum chamber to prevent the accumulation of oil molecules was an effective method to prolong the life of the Cathode ray tube.

D. Measurement Equipment

1. Capacitance Bridge

A General Radio Capacitance-Measuring Assembly Type 1620-A was used to measure the capacitance and loss tangent of samples. This assembly consists of the Type 1615-A Capacitance Bridge with the Type 1311-A Audio Oscillator and Type 1232-A Tuned Amplifier and Null Detector. This bridge is designed to cover a range from 20 HZ to 100 KHz, direct by reading in capacitance at any frequency and in dissipation factor at 1 KHz with correction factors for measurement at other frequencies. It covers a capacitance range of 10 pf to a maximum of 1 μf, with internal standard capacitor, and achieves an accuracy of ± 0.1%.

The coverage of the dissipation factor is from 1 PPM to 1 with an accuragy of ±(0.1% + 10 PPM) at 1 KHz. The samples were put in a shielding jacket and co-axial cables were used to connect the sample to the bridge. The cables were kept as short as possible but the lead capacitances were still significant. It was measured to be about 8 pf and was subtracted from the capacitance reading.

In all measurement, the input signal was kept 0.1V to assure the field more than two orders of magnitude below breakdown level and consequently, measurements should be possible without any chance whatever of incipient breakdown or ionization phenomena. Both capacitance and dissipation factor were measured to four significant figures.

The bridge measures the capacity and dissipation factor of an equivalent parallel combination of capacitance and resistance. Since the sample is equivalent to parallel capacity and resistance no correction is necessary.

2. Constant Temperature Chamber

Two Delta Type 1060L constant temperature chamber were used to keep samples at constant temperature for aging effect tests. The measurement of capacitance and loss tangent of samples at different temperature also were done by putting the samples with the shield jacket in the chamber to heat up to desired temperature, the actual temperature of the samples was monitored by attaching a pair of thermocouples in close vicinity to the capactor plate on the substrate. A pair of co-axial cables provided the connection between sample and the bridge.

The chambers with the built-in heat source provided the constant temperature range from room temperature (about 25°C) to 250°C with ± 2°C accuracy at the center of the chamber. The temperature was set by means of meter-operated automatic control.

3 Resistance Bridge

The resistance bridge which could simultaneously measure the current and voltage of the sample was used for dc conductivity and dielectric strength measurements. The bridge is balanced at open circuit. As showed in Figure-6 the input impedance of volt meter Vm2 serves as one arm of the bridge. The bridge becomes unbalanced when an unkown resistance is placed in the circuit. The unbalanced voltage, 1/4, as read by a voltmeter, Vm1 and is proportional to the current through the specimen, I_s. The current is given by[19]

$$I_s = 1.13 \times 10^{-5} V_4 \text{ amps}$$

Current of 10^{-12} amps may be measured in specimens from 10K to 10 meg ohms with accuracy better than 5%.

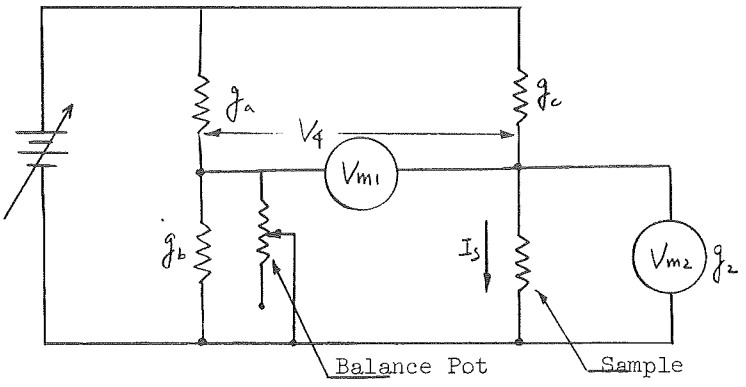

Figure 5 Resistance Bridge

CHAPTER IV

EXPERIMENTAL RESULTS

A. Introduction

More than sixty metal-polymer-metal structures have been constructed for various measurements. During the deposition of the polymer layers, all parameters were closely monitored and recorded to establish the order of these affects and to provide a common basis of comparison for all of the specimens. Measurements of capacitance and dissipation factor were made on all specimens immediately after they were constructed and finished as soon as possible to avoid aging effects. Exposure of specimens to air invariably resulted in remarkable decreases of capacitance. Measurements were made for a series of specimens over a range of frequencies or over a range of temperature, but more attention was devoted to the measurements at room temperature over a range of frequencies. Long term aging effects on dielectric properties have also been observed.

Several subtle steps had to be adopted both in the construction and measurements procedure. This was time-consuming and tend to limit the number of specimens which could be handled. About one half of the specimens fabricated yield significant data which is much more than enough for analysis. The polymer films analyzed, otherwise noted, are formed at system pressure of 5×10^{-4} to 4×10^{-5} torr at room temperature with an electron beam current density of 10.2 $\mu A/cm^2$ at 360V.

B. Film Growth

Several polymer films have been formed under identical system pressure

and current density but with different accelerating voltage, no dependence of growth rate on accelerating voltage was observed in the range of 300V to 600V, however, it is found that the films formed at higher voltages up to 660V had much higher dissipation factor. Because of this effect, the accelerating voltage was fixed at 360V for most specimen. Christy's[6] phenomenological formula predicted the linear dependence of growth rate on current density at this low current density, but the experiment showed a contrary result. It can be seen from Figure-6, lowering the current density 25% decreased the growth rate by half. The growth rate was a fairly linear function of time for both cases, and was calculated to be 4.2 Å/min for current density of 10.2 $\mu A/cm^2$ at room temperature.

Most times the extra source was heated to and kept at 60°C for more than one and an half hours before film was deposited. It is found that the system had already reached saturation condition at this times, because no increase in growth rate was observed by turning on the heater of the extra source for a much longer time before deposition.

It seems to be impossible to deposit polymer films of desired thickness with high accuracy only by controling the deposition parameters and deposition time. Other monitoring techniques such as microbalance technique should be employed.

C. A.C. Measurements

1. Dielectric Constant

In this experiment thicknesses of most films were indirectly determined by capacity measurement, and thus the dielectric constant should be

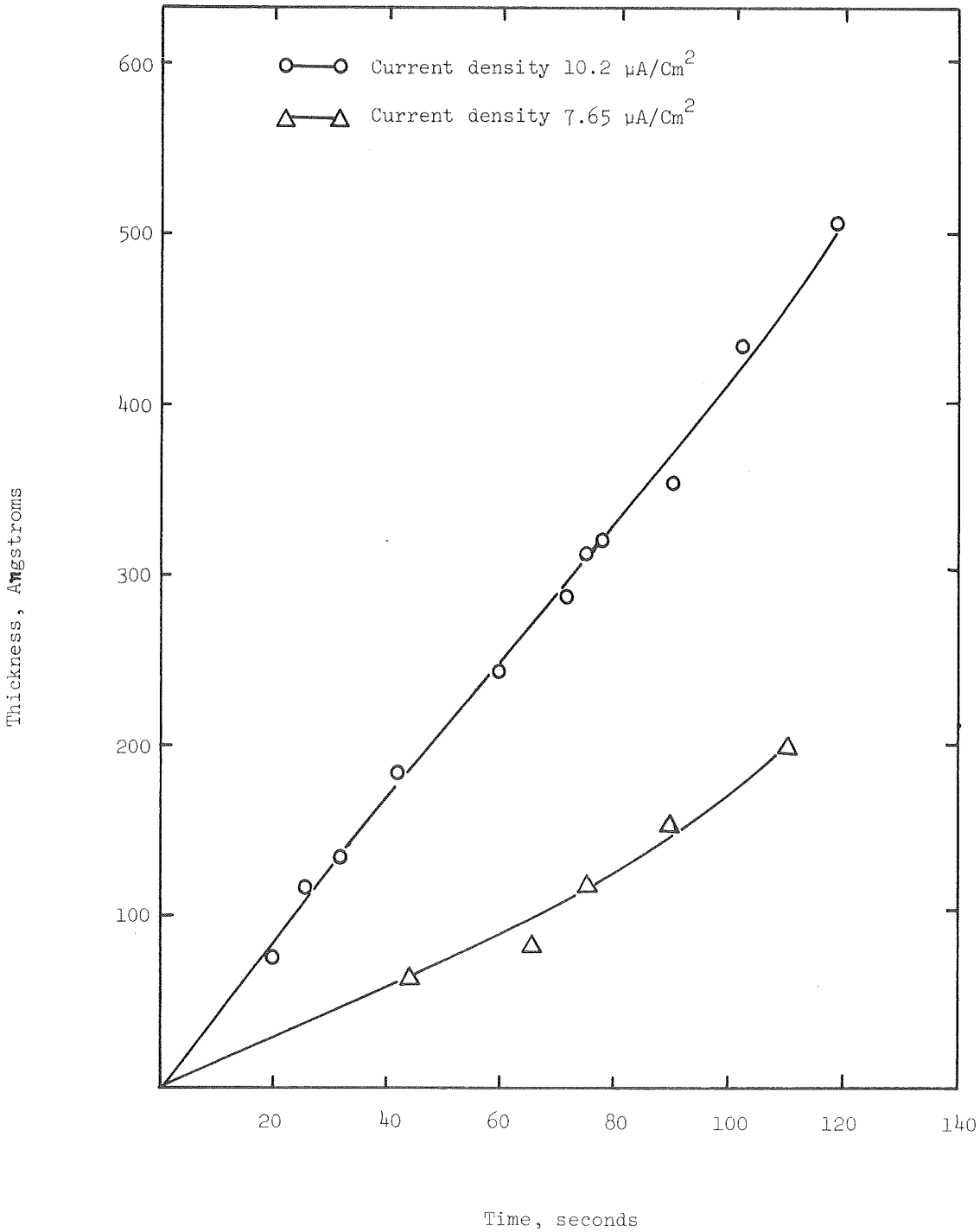

Fig - 6. Film Growth

known with sufficient degree of accuracy. Previous work[6,5,19] showed that the relative dielectric constant to be 2.8 at 1 KHz. Thicknesses of three specimens have been determined by ellipsometric measurement with an estimated accuracy of ± 5Å. Within experimental error, the relative dielectric constant calculated from the measured thicknesses and capacitances consistantly fell on the same value of 2.8 at 1 KHz. This value seems to be reliable.

Ellipsometric measurement along with an extensive computer program was employed to calculate the index of refraction of the polymer films. The results showed that the index of refraction of the polymer films is 1.39 and that the optical dielectric constant is 1.93. This value is somewhat lower than that of 1.6 to 1.8 estimated by Christy[6].

2. Dielectric Relaxation

Dielectric constant and dissipation factor measurement over a frequency range of 0.2 to 100 KHz were made for all the specimens. The measurements were made in open air immediately after the specimen was moved out from the vacuum chamber and completed as quickly as possible and usually required no more than an hour to complete. The changes in capacitance and dissipation factor due to aging effect could be neglected.

The results obtained for specimens of various thickness fell in the same pattern. Figure-7 shows the percent changes in capacitances against frequency for four specimens and the corresponding curves for dissipation factor are showed in Figure-8. Curves in Figure-7 showed a steady decrease in capacitance with an increasing frequency within the measuring range. The rate of change is rapid at the low-frequency and a consistent change of slope of curves occurs between 3 and 4 KHz, decreasing the rate of change. The changes in ε' are between 4.5% to 8.7% for the range of 0.2 to 100 KHz.

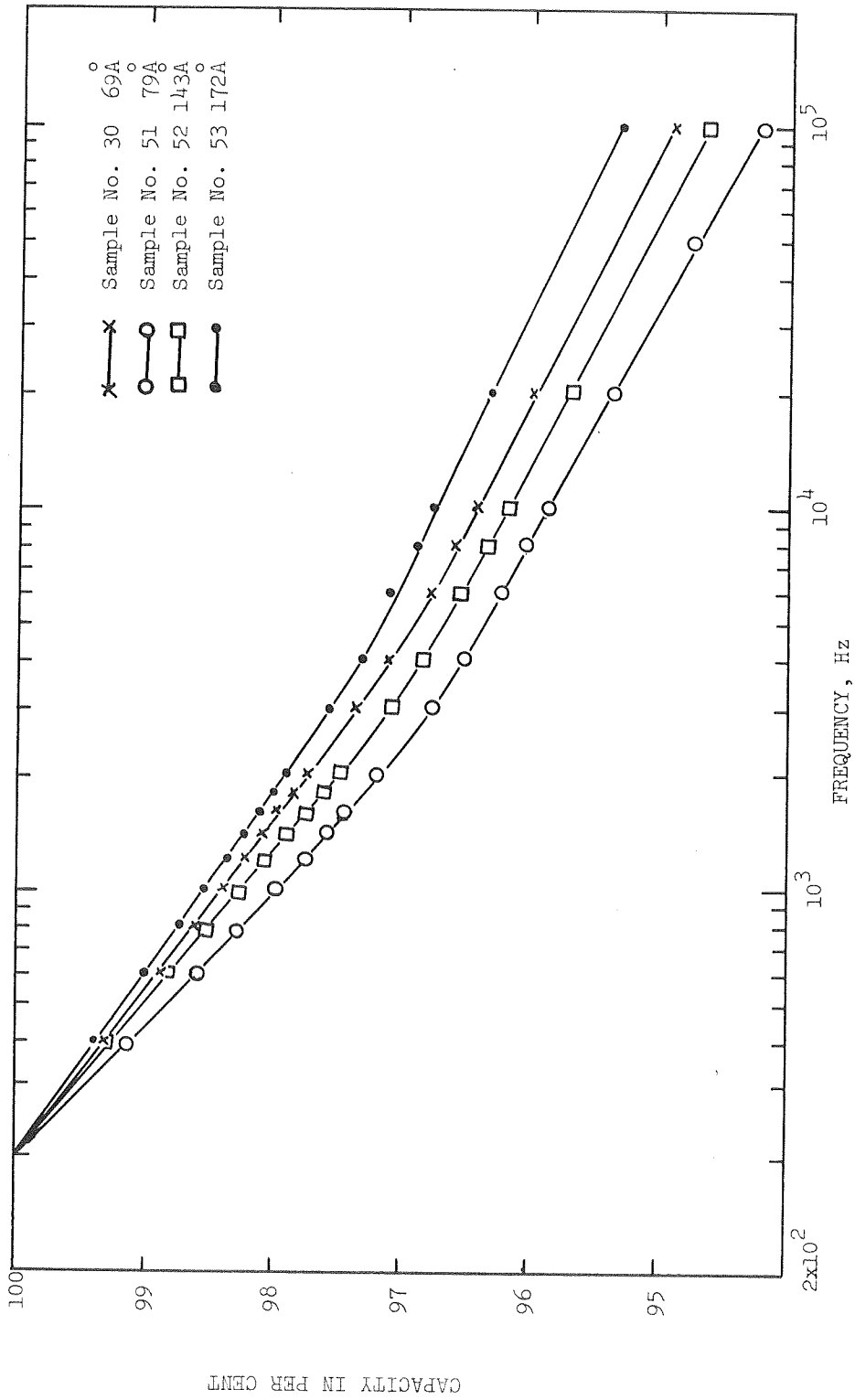
Sample No. 30 69A°
Sample No. 51 79A°
Sample No. 52 143A°
Sample No. 53 172A°
CAPACITY IN PER CENT
100
99
98
97
96
95
2x10^2
10^3
10^4
10^5
FREQUENCY, Hz

Fig - 7.

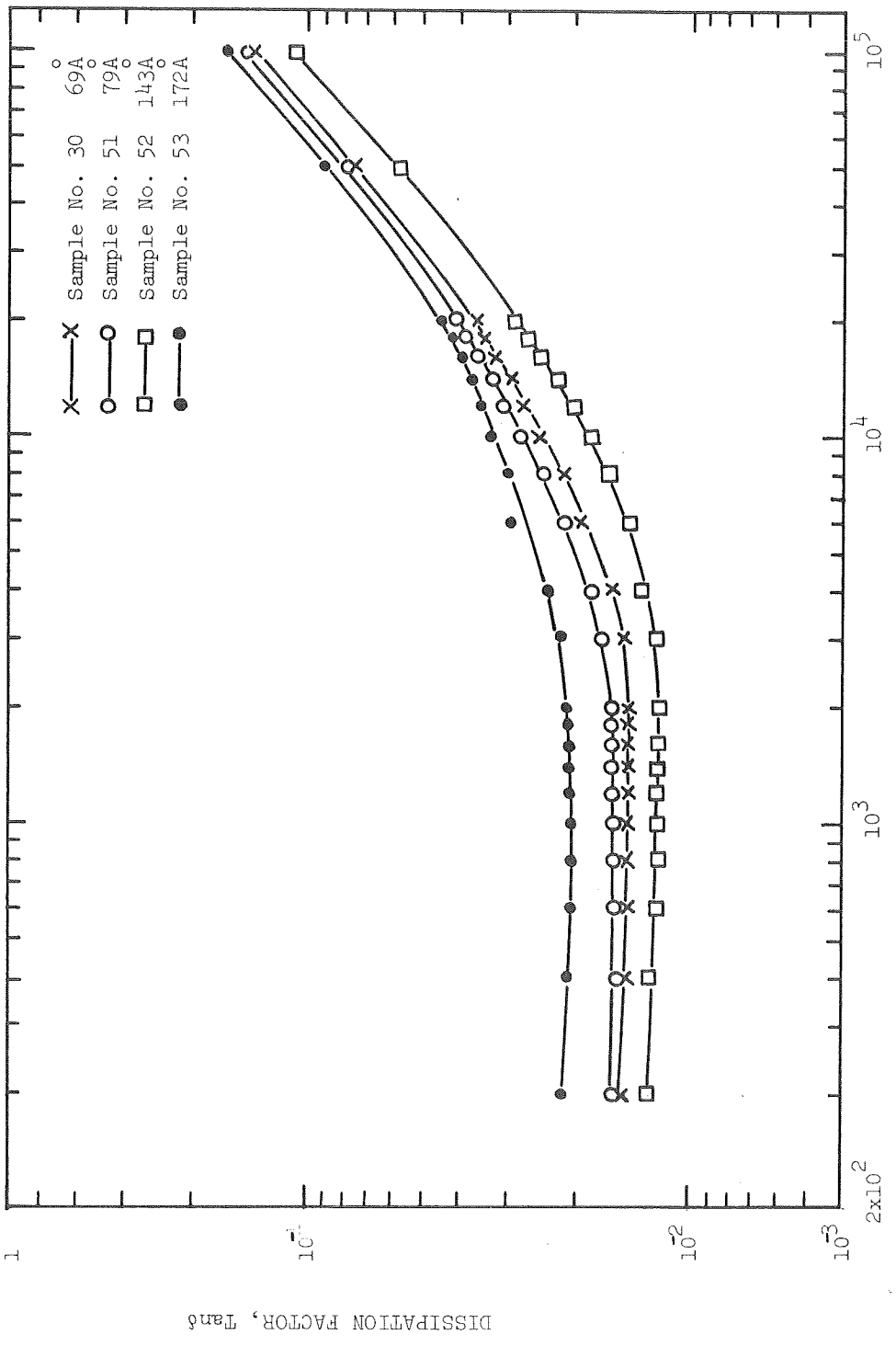

Fig - 8. Dissipation factor vs. Frequency for Samples of Different Thickness

As can be seen in Figure-8 the losses of this polymer generally tend to be one to two orders of magnitude higher than that expected for common polymers. Initially the dissipation factor decreases slightly with increasing frequency up to 2 KHz and then increases sharply towards the high-frequency end of the range. There is no loss peak within the range of frequencies observed but the shape of the dissipation factor curves, in conjunction with the corresponding capacitance curves in Figure-7 suggests a loss peak above 100 KHz and outside the range of the measurement. If the results are explained in terms of a high-frequency loss peak, it must lie at a frequency much higher than 100 KHz. The deviation in dissipation factor indicates a considerable variation of material properties among the four specimens. This is not unexpected for heterogeneous solids.

The detailed data available shows no evidence for correlating the variation of both capacitance and dissipation factor with frequency to the thickness of the specimens.

3. Modified Cole and Cole Plot

In an effort to characterize the polymer films, models have been developed for analysis. The results to be presented are representative but have been chosen so that the same model can be used for most specimens in a good agreement with the experimental data.

The changes in capacitance and dissipation factor with frequency for a typical specimen are showed in Figures 9 and 10. The corresponding curves for ε' and ε'' are showed in Figure 11. The shape of dissipation factor suggests that there is a loss peak above 100 KHz. The plot of ε' and ε'' on complex plane (Figure 12) tend to support this suggestion and suggest another possible peak below 200 Hz. Without knowning actual mechanisms which contribute to the losses,

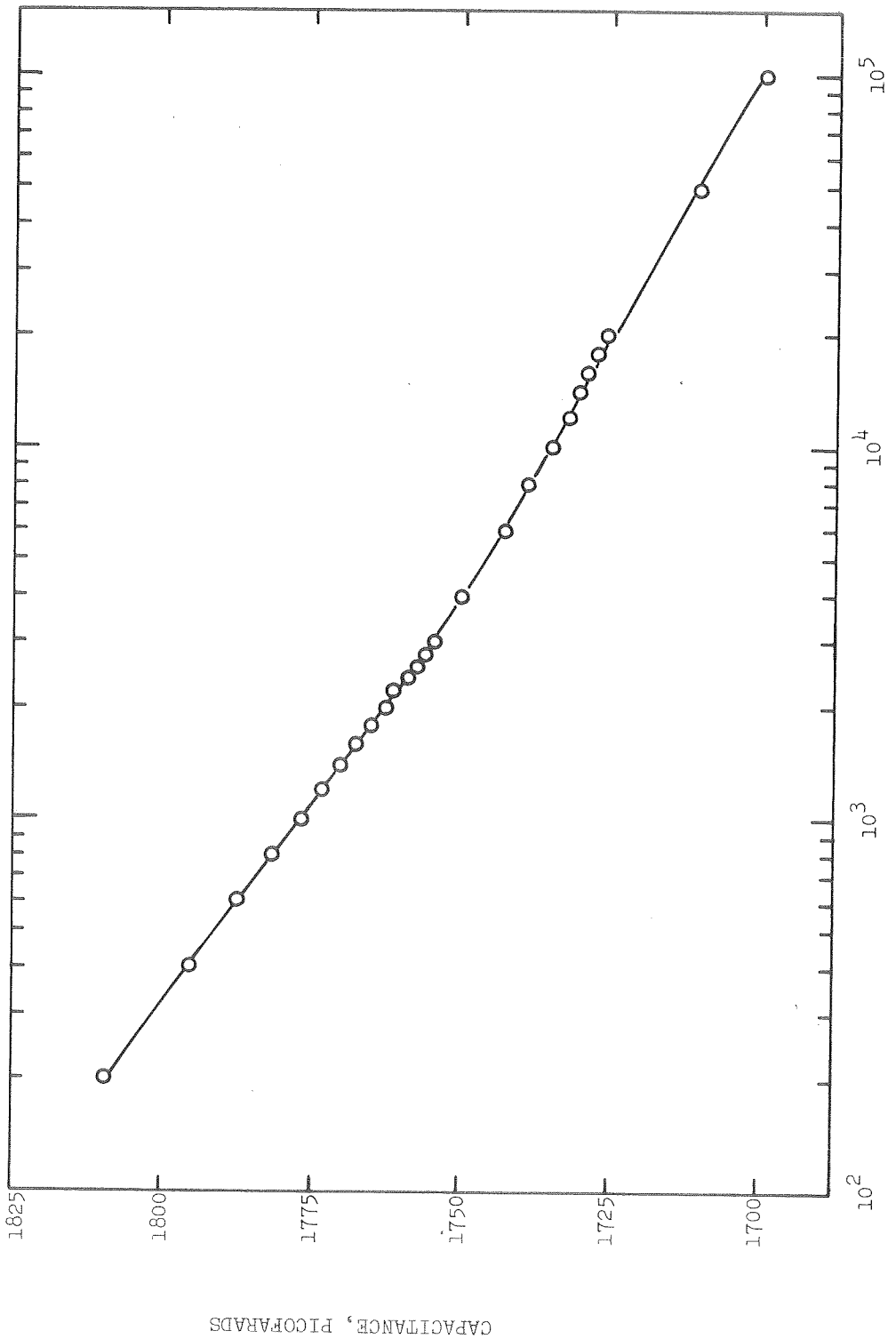

Fig - 9. Capacitance vs. Frequency for Sample No. 18, 178$\mathring{A}$

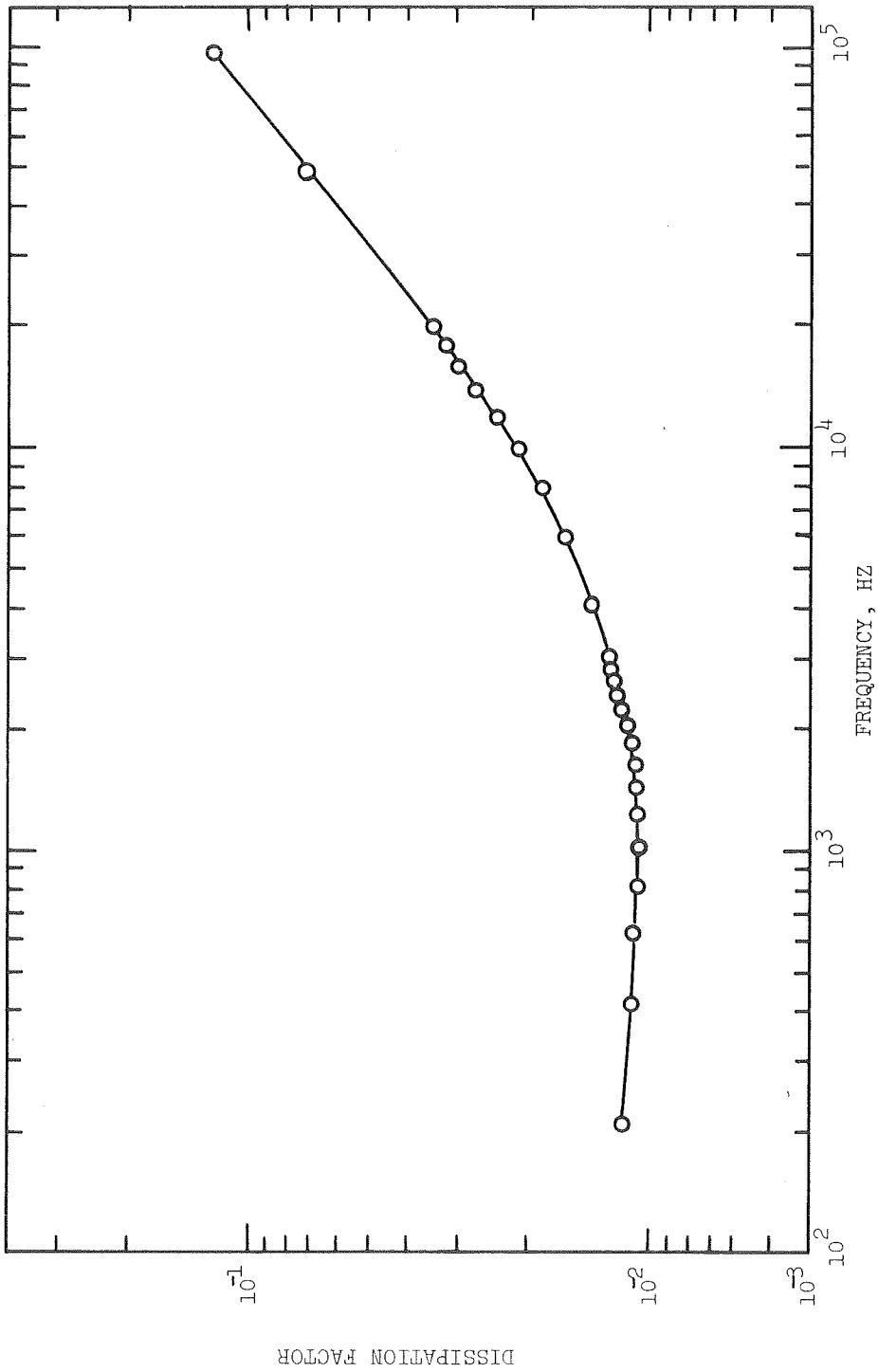

Fig - 10. Dissipation Factor vs. Frequency for Sample No. 18, 178 Å

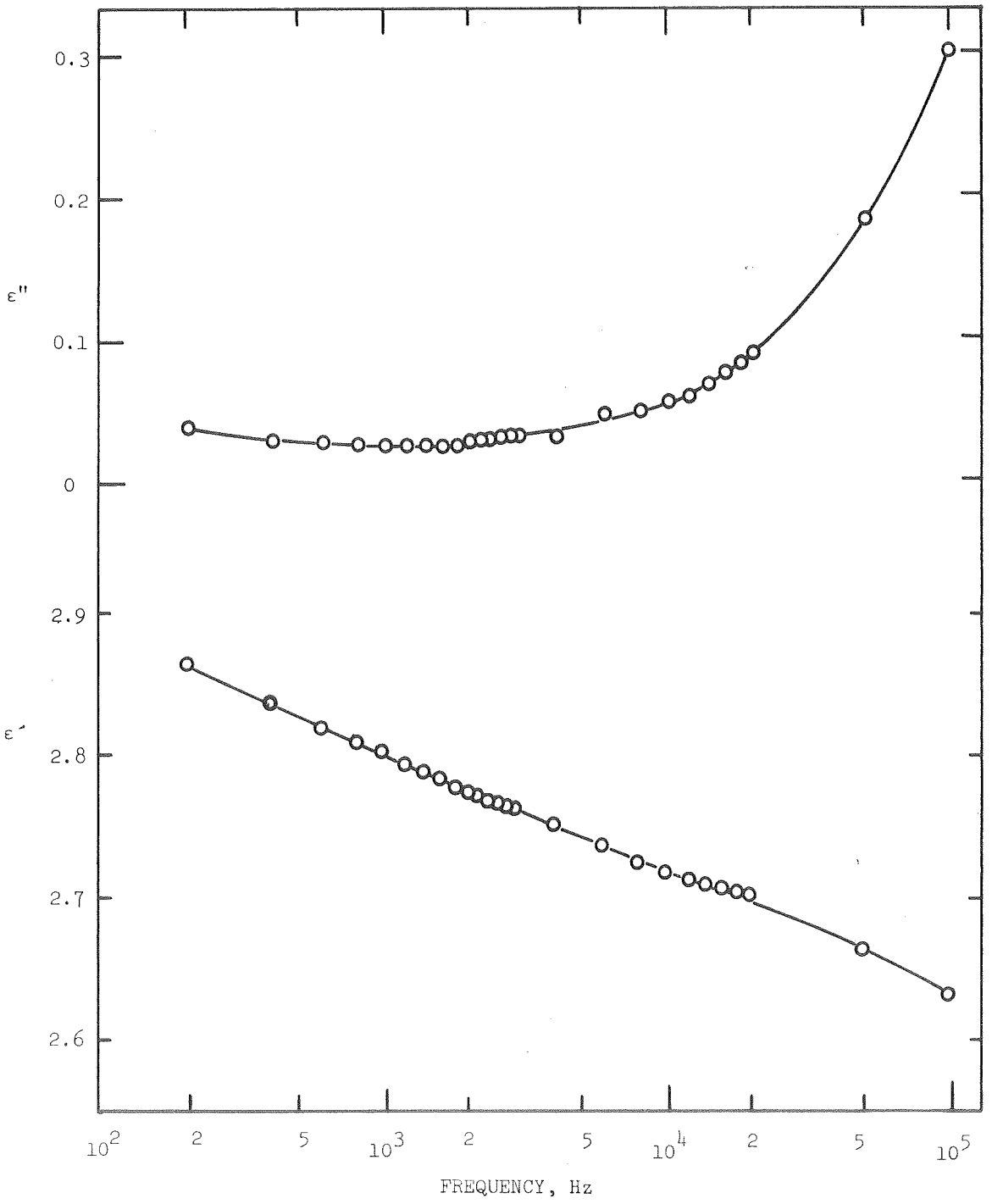

Fig - 11. ε" vs. Frequency and ε´ vs. Frequency for Sample No. 18 178Å

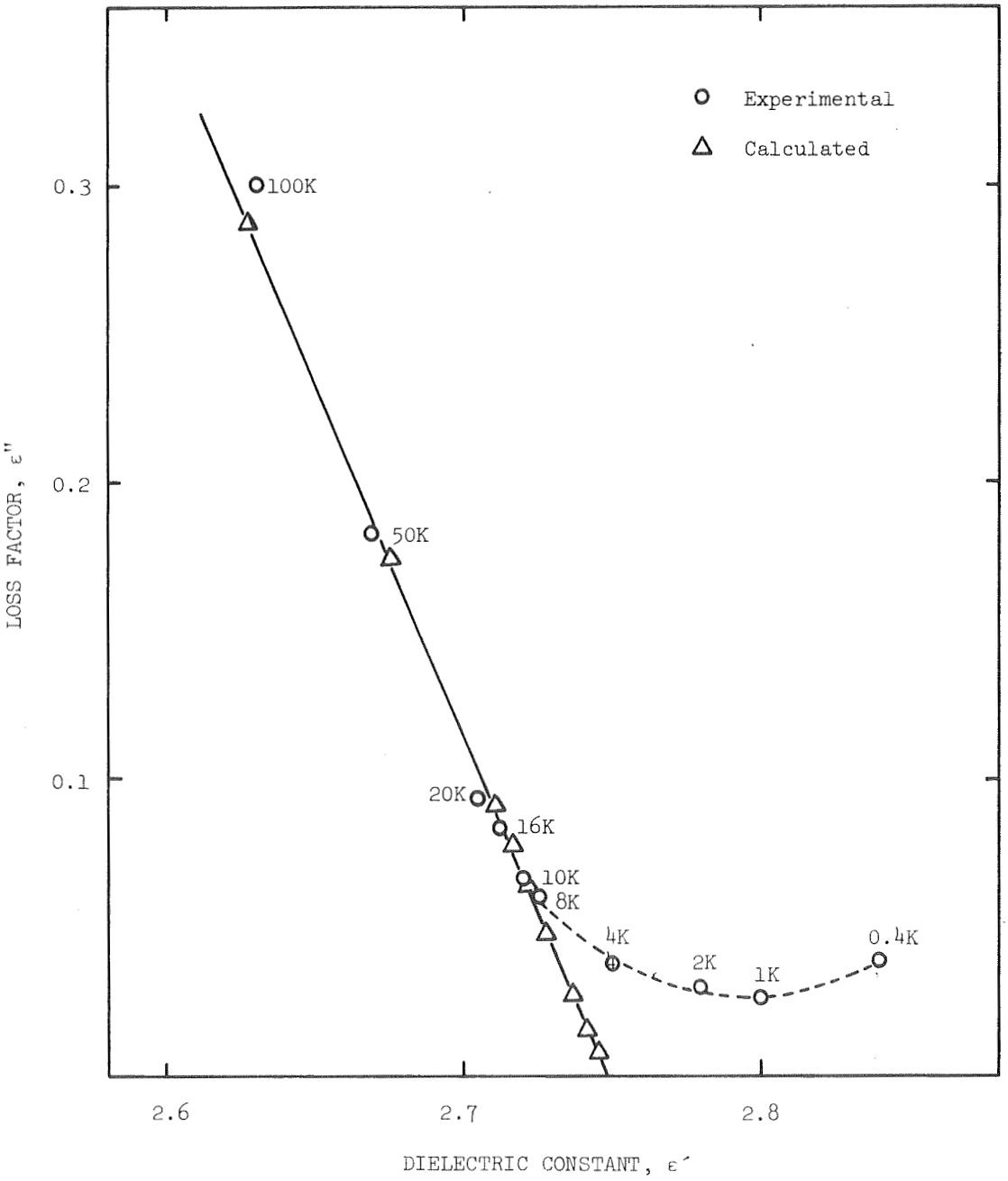

Fig - 12. Loss Factor vs. Dielectric Constant for Sample No. 18 178A°

we assume that there are dipole-like relaxations with two dispersion regions in the polymer films and employ Eq. 38

$$\varepsilon^* = \varepsilon^\infty + \frac{K_1}{1 + (j\omega\tau_1)^{1-\alpha_1}} + \frac{K_2}{1 + (j\omega\tau_2)^{1-\alpha_2}}$$

Let τ_1 and τ_2 be the most possible relaxation time for high frequency and low frequency dispersion region respectively then the measured frequency will fall into the two regions (c.f. Figure 13)

(a) $\omega\tau_1 << 1 \qquad \omega\tau_2 \simeq \infty$

For this case Eqs. 39 becomes

$$\varepsilon^* = \varepsilon^\infty + K_1 + K_1 (-j\omega\tau_1)^{1-\alpha_1} \tag{39}$$

It can be written as

$$\varepsilon' = \varepsilon^\infty + K_1 + K_1 (\omega\tau_1)^{1-\alpha_1} \text{ Sin } (\frac{\pi\alpha_1}{2}) \tag{40}$$

and

$$\varepsilon'' = K_1(\omega\tau_1)^{1-\alpha_1} \text{ Cos } (\frac{\pi\alpha_1}{2}) \tag{41}$$

with $o < \alpha_1 < 1$

(b) $\omega\tau_1 = o \quad \omega\tau_2 >> 1$

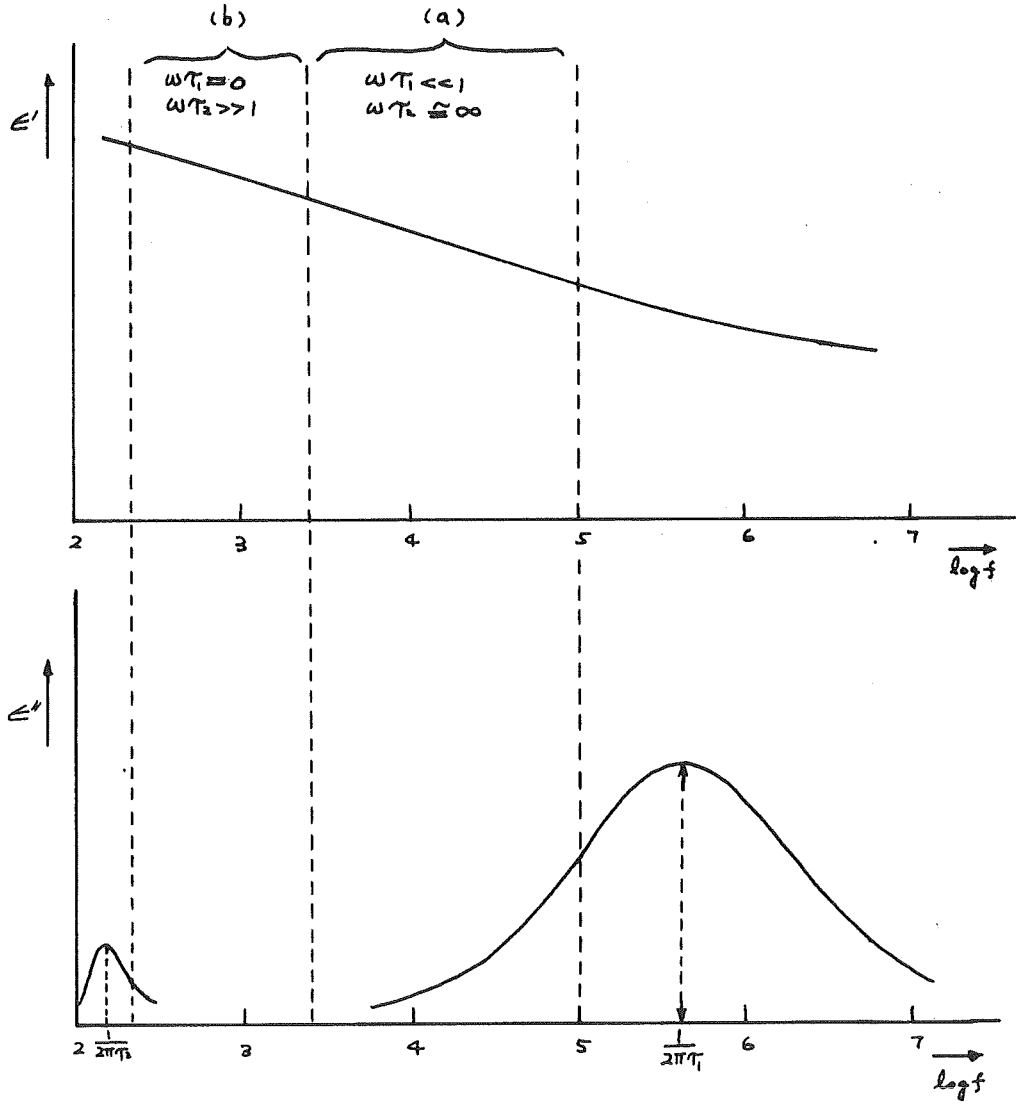

Fig - 13. Two Dispersion Regions for Polymer Film.

This gives

$$\varepsilon^* = \varepsilon^\infty + K_1 + K_2 (\omega\tau_2)^{(\alpha_2-1)} e^{-(\frac{\pi}{2})j(1 - \alpha_2)} \tag{42}$$

and can be written as

$$\varepsilon' = \varepsilon^\infty + K_1 + K_2 (\omega\tau_2)^{(\alpha_2-1)} \text{ Sin } (\frac{\pi\alpha_2}{2}) \tag{43}$$

and

$$\varepsilon'' = K_2(\omega\tau_2)^{\alpha_2-1} \text{ Cos } (\frac{\pi\alpha_2}{2}) \tag{44}$$

with

$$o < \alpha_2 < 1$$

Except for frequencies below 2KHz, in most portions of the observed frequency range, the real dielectric constant, ε' was observed to decrease steadily with increasing frequency while over the same range the loss factor ε'' increased with increasing frequency, Eqs (40) and (41) can be used to express these features for a dispersion and obsorption region with a loss peak at frequency about 100 KHz.

In the frequency region below 2KHz, the real dielectric constant, again decreased with increasing frequency, but the loss factor ε'', was observed also to decrease with increasing frequency. These features are consistent with Eqs. (43) and (44) for a dispersion peaking at frequency below 200Hz.

Because of the restriction of the frequency range, capacitance and dissipation factor measurements could not be make for frequencies below 200 Hz, without sufficient information, it would be inexpedient to analysis the low frequency dispersion and thus the effort was devoted mainly on the high frequency dispersion. Eqs. (39) and (40) were chosen for comparison with experimental data. Figure 13 shows the experimental curves for specimen number 18 (178 Å) and the calculated curve with $K_1 = 1.2$, $\alpha_1 = 2.6$, $\varepsilon^\infty + K_1 = 2.75$, the agreement is quite good from 8 KHz up to 100 KHz. Using the appropriate values the approximate value for the realxation time τ_1 is found to be 2.7×10^{-7} sec (loss peak at 590 KHz).

Five specimens thickness from 79 Å to 285 Å were used for further analysis, the results showed that roughly the same high frequency characteristics existed in every specimens with a superimposed low frequency dispersion. The parameter α_1 differs from specimen to specimen, ranging from 0.22 to 0.31. The larger value of α_1 represented a broader distribution of relaxation times. Average value for static dielectric constant $\varepsilon^\infty + K_1$ for the polymer films is found to be 2.73 ± 0.08 and τ_1 is found to be between 1.9×10^{-7} and 4.5×10^{-7} sec.

The deviation in these parameters provided the evidence for considerable deviation in material properties among these specimens. Due to lack of sufficient knowledge of the polymer film structure, no conclusion could be drawn to underly the reason for this spread of values.

4. Aging Effects

During the early experimental work[5,8] small increases in capacitance and dissipation factor with time were observed when the specimens were stored in room air. The change in capacity was attributed[8] to the increases in dielectric constant by the saturation of long-lived phenyl free radicals formed during the polymerization process, and the saturation was carried out absorption of atmospheric water.

For aging effects observations, more than twenty specimens were made and stored in atmospheric air. Capacitance measurements were made at 1 KHz immediately after the specimens were moved from the vacuum chamber and then made periodically in open air. It was found that none of these specimens had showed increases in capacitance or dissipation factor for two week, contrary to the findings of others.

All the specimens showed a decrease in capacitance during the first three days and the aging curves tended to flatten out thereafter. The capacitance apparently became stable after twenty days. A plot for six of the specimens is given in Figure 14. Figure 15 shows the percentage decreases of capacitance against time for specimens of different thickness. It can be seen from these curves that the resultant percentage decrease of the capacitance is proportional to the thickness of the specimens. Since all the specimens have been normalized to the same area, from a phenomenological point of view, the decrease in capacitance seem to be a bulk function rather than a surface function. The corresponding resultant percentage decrease in capacitance is plotted in Figure 16, as a function of thickness. A fairly good straight line relation is obtained and hence the slope of the plot gives the resultant percentage capacitance decreases of the specimens. The resultant percentage change is approximately

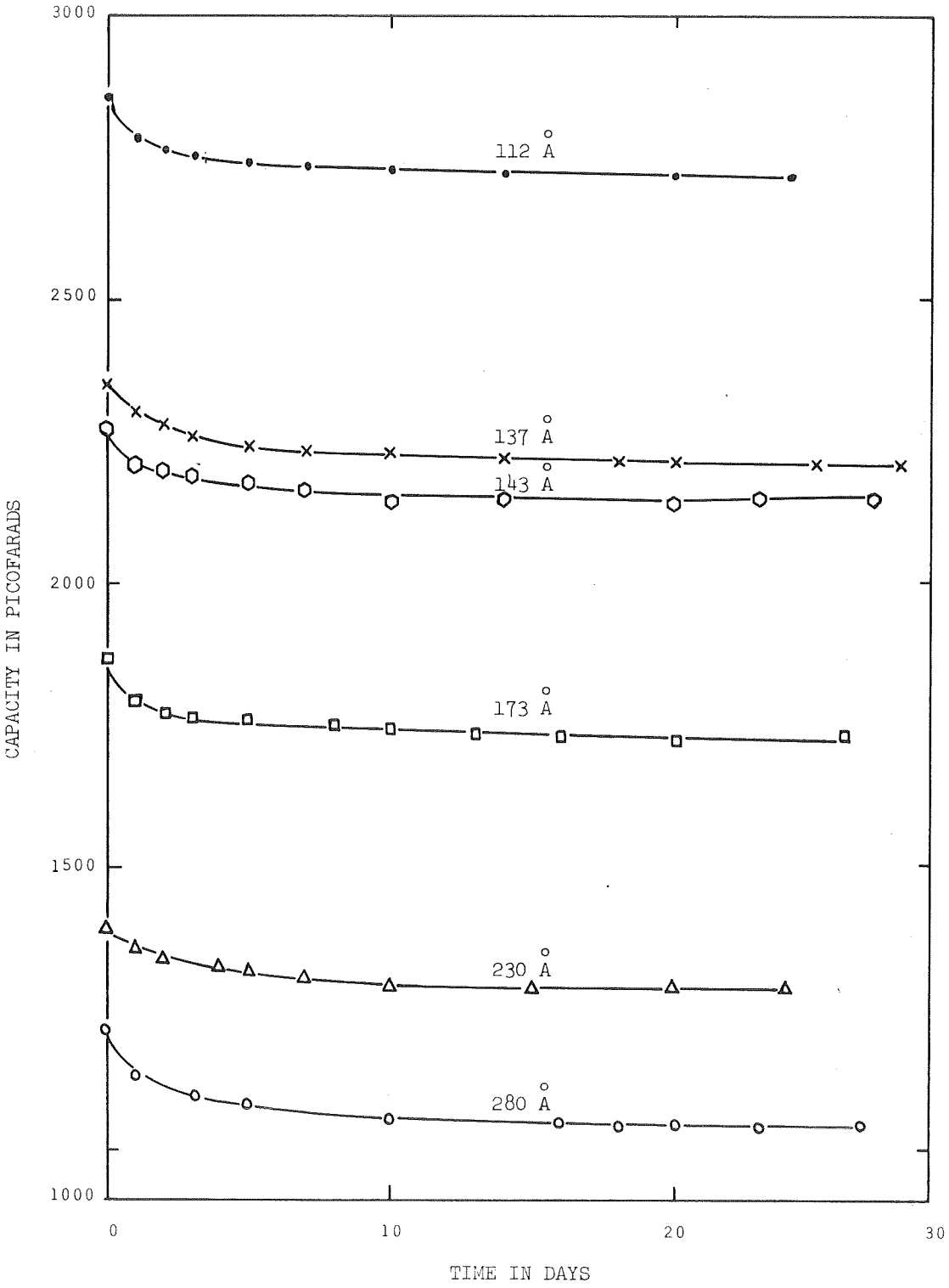

Fig - 14. Capacitances vs. time for samples of different thickness at 1 KHz (all current normalized to a 1.3 mm^2 area)

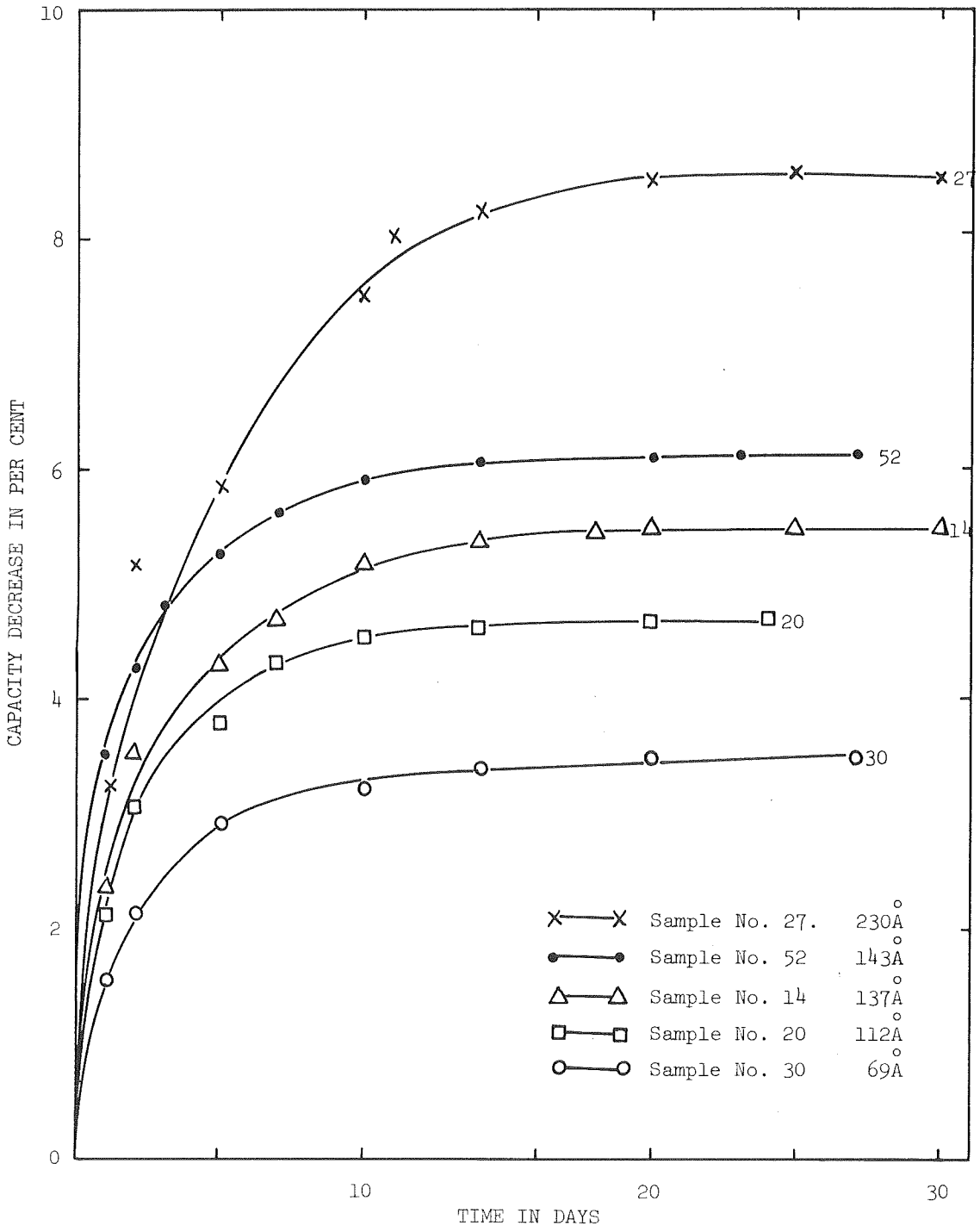

Fig - 15. Per cent decreases of capacitance vs. time for samples of different thickness at 1 KHz

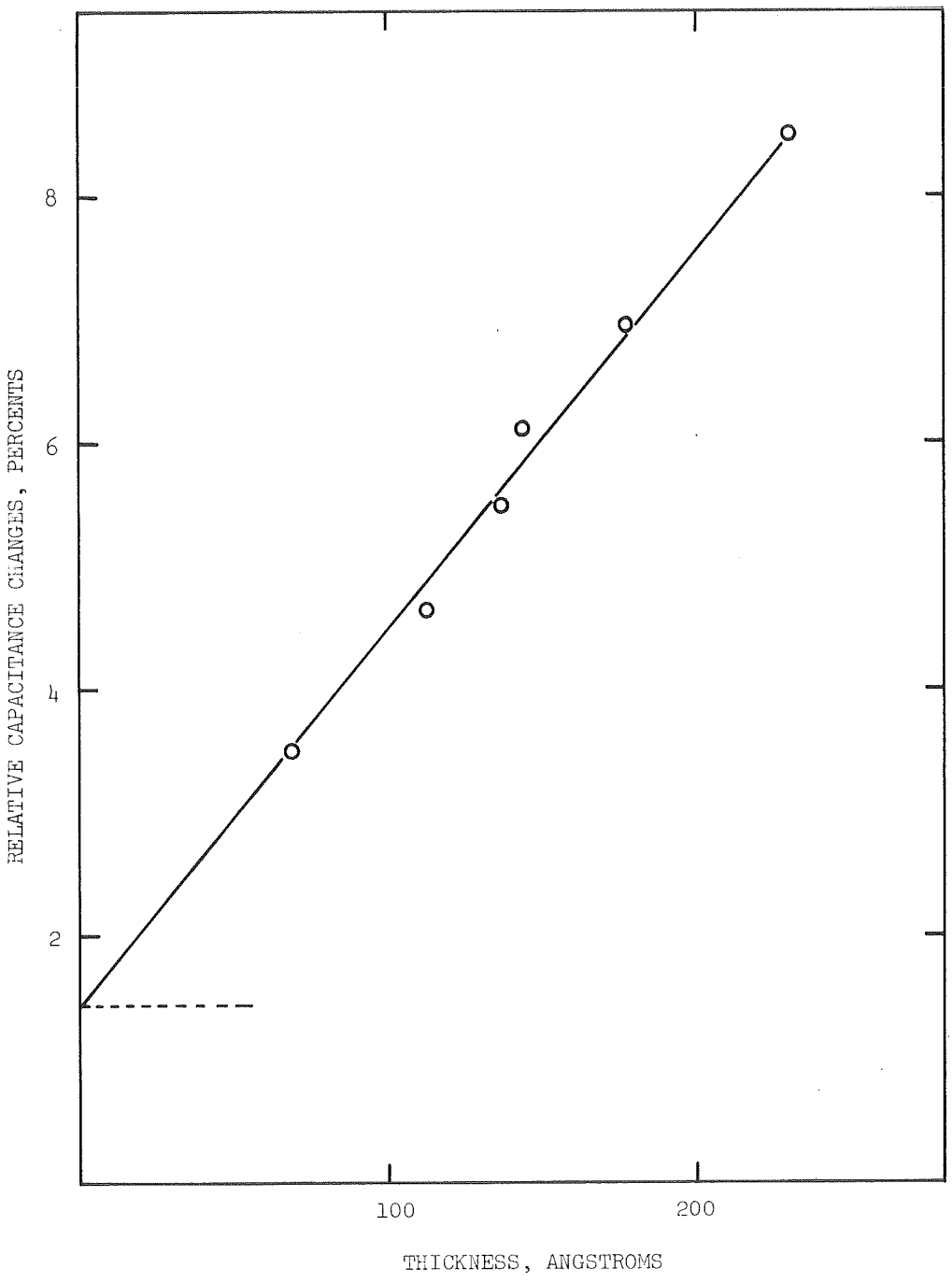

Fig - 16. Resultant percentage Capacitance Changes vs. Thickness at 1 KHz

given by

$$\frac{\Delta c}{c} \ (\%) \ = \ 1.45 + 0.03d \qquad (45)$$

where d is the thickness of the specimen in angstroms.

The changes in dissipation factor deviated from sample to sample, however, Figure 17 shows the results which are quite typical. All the aging curves fell sharply in the first three days but little change was observed during the successive week. The dissipation factor then increased continuously to a value higher than the initial value and became more stable. It is worth noting that both the capcitance and dissipation factor come to the steady state values after same period of aging even though they follow quite different patterns.

Two additional specimens were stored in vacuum at 5×10^{-4} to 10^{-5} torr for five days, no significant changes in capacitance or dissipation factor were noticed. Three additional specimens were stored in dessicated air for three weeks, the capcitance and dissipation factor were then measured. Their capacitance decreased with time like those stored in room air, but the dissipation factor changed drastically. Furthermore, if the moisture was taken up by the film, both the capacitance and dissipation factor should have increased. This did not fit the experimental facts, which showed decreases in both capacitance and dissipation factor during aging in room air. One cannot immediately interpret the changes in capacitance and dissipation factor is due to the absorption of water vapor as concluded by other workers.[5,8] Alternaltively, it might be suggested that these changes are due to the absorption of oxygen into the film.

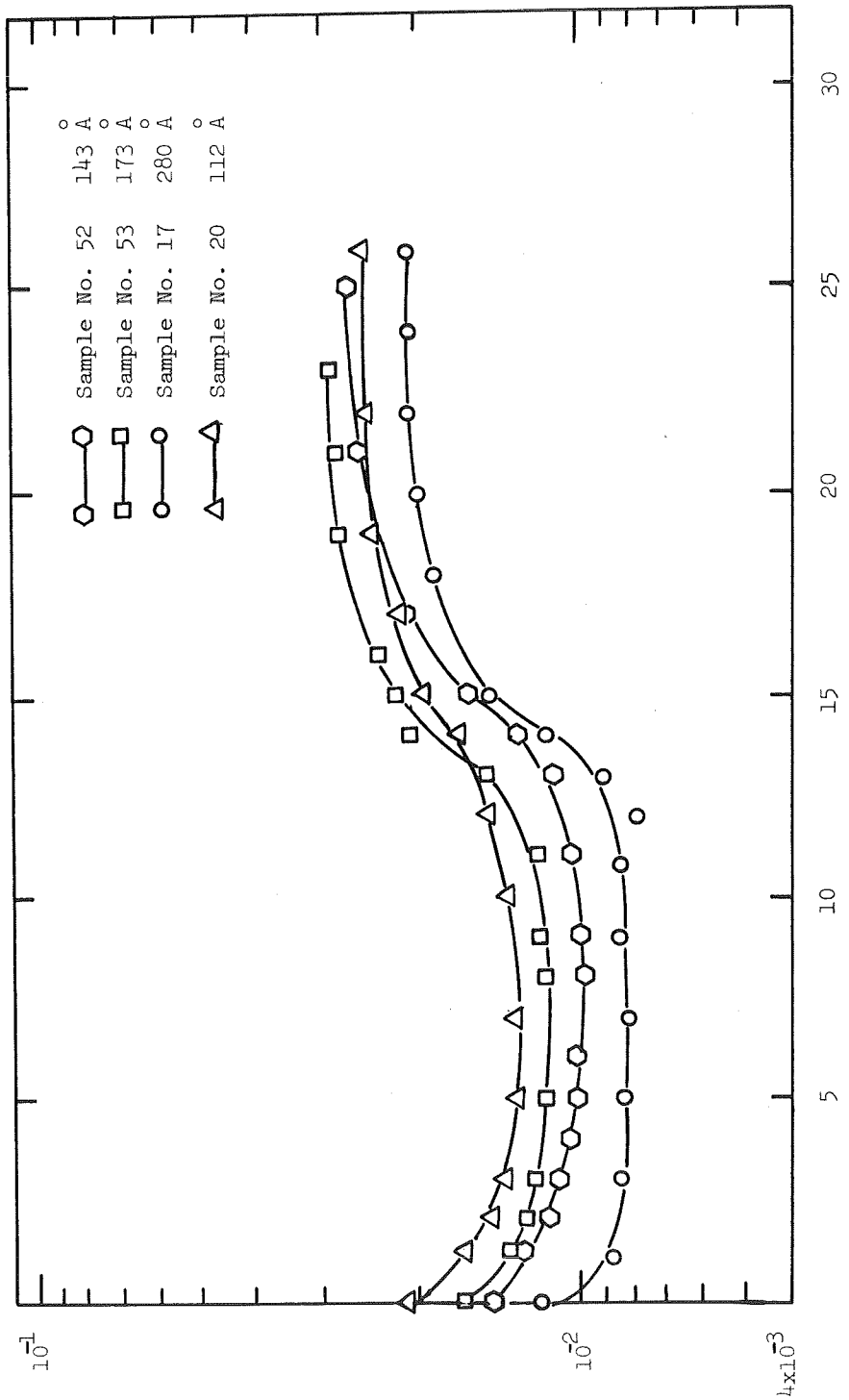

Fig - 17. Dissipation Factor vs. Time for Samples of Different Thickness at 1 KHz

Regardless of the actual mechanism, at this stage, a reasonable conclusion can be drawn from Figure 16. Since the capacitance of a specimen is given by

$$C = \frac{\varepsilon \varepsilon_o A}{d}$$

Where C is capacitance, ε is the relative dielectric constant of film ε_o is the dielectric constant of vacuum, A is the area of the specimen, and d is the thickness of the film. For a fixed area, only an increase in d or a decrease in ε, or both can result in decrease in capacitance. It has been observed that, for a specimen stored in room air for a period, more voltage was required to maintain the same current, i.e. a decrease in electron transport current. It suggests an increase in thickness. These results are, however, in agreement with the suggestion that the decreases in capacitance are due to the increase in film thickness.

Hill[8] working with polymethlsiloxane films, observed a decrease in capacitance for specimens stored in atmosphere and attributed the changes to the desorption of trapped high vapor pressure unpolymerized monomer from the polymer films which were formed by the low energy electron beam bonbardment.

For specimens produced by higher energy(700 eV or higher) electron beam bonbardment, similar aging effects are observed. Their curves of capacitance changes against time fell in the general pattern established for those formed by 360 eV electron beam. The only significant difference is that the resultant percentage changes of capacitance of these specimens are somewhat lower than that predicted by Eq. 45. This suggest that the resultant percentage changes

of capacitance depends on the energy of formation and tends to decrease for higher energy of formation. These effects obviously need to be observed in more detail.

5. Temperature Dependence

Temperature dependence of the capacitance and dissipation factor were investigated by keeping specimens at different temperature and making measurement over a frequency range from 0.2 KHz to 100 KHz. For every specimen pronounced increases in capacitance with increases temperature were noticed. The temperature dependence of capacitance at 1 KHz for two specimens are illustrated in Figure 18. Figure 19 represents plots of ε' and ε'' against frequency for specimen number 48 at temperature as indicated. From the plots of ε'' the suggested high frequency loss peak apparently tended to shift to higher frequencies with increasing temperature. Figure 20 shows the corresponding modified Cole and Cole plots. From the asymptotes of the plots, it can be found that the Cole and Cole parameter α_1 for the suggested high frequency dispersion is slightly decreasing with increasing temperture. Since the parameter α_1 reflects the width of distribution of relaxation times, and thus the decrease in α_1 with time indicates a narrower distribution of relaxation times at higher temperature.

The increase in capacitance at elevated temperature has been attributed to a decrease in the equivalent parallel resistance of the sample, this results in a increase in measured capacitance.[41] Unfortunately, there is not sufficient knowledge of the film structure to confirm this interpretation and support a model for the spread of this parameter.

6. Effects of Voltage on Capacitance

The capacitance measured with a small ac field depends very pronouncedly on any dc bias voltage present. The percent change in capacitance

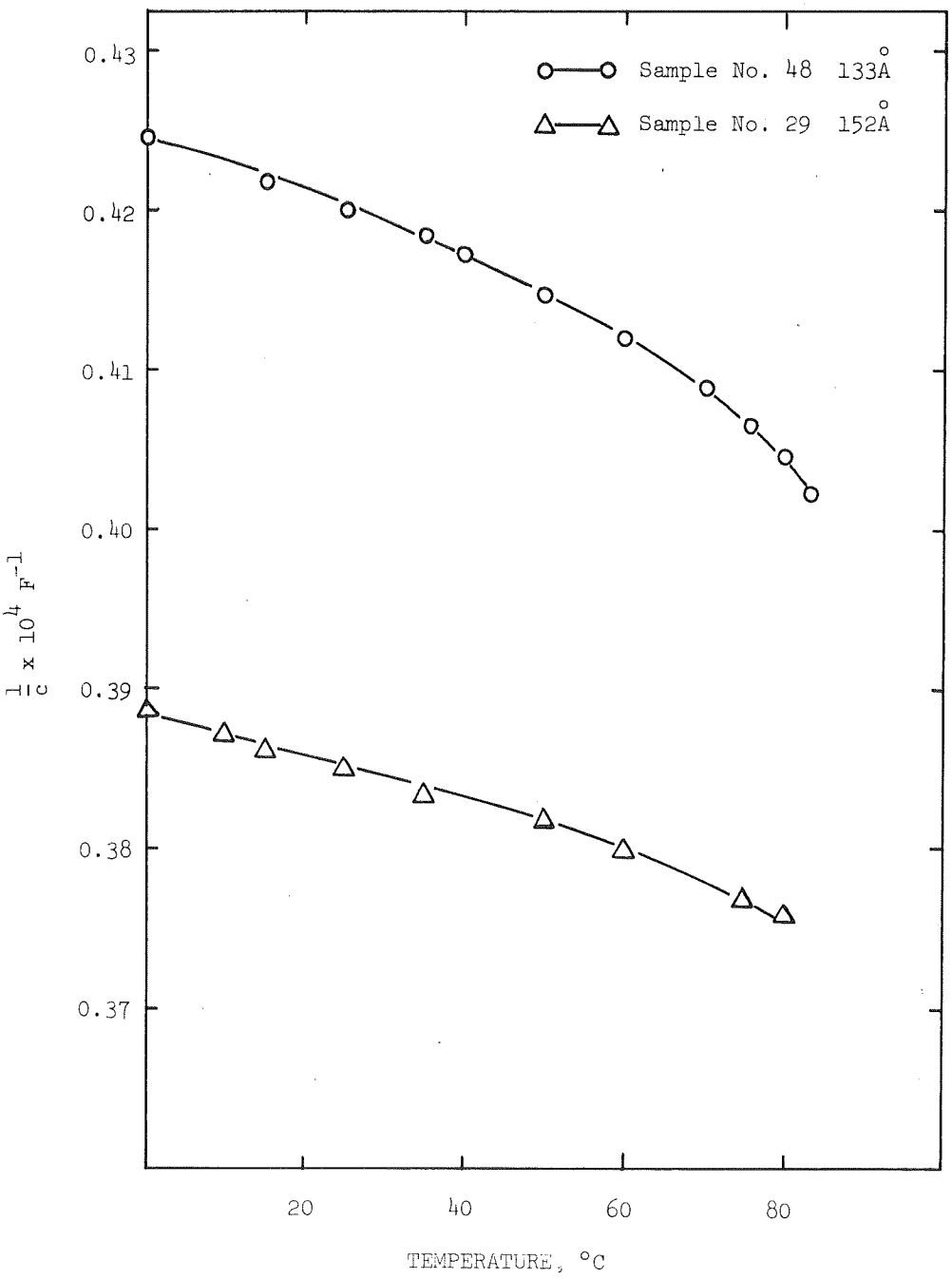

Fig - 18. Inverse Capacitance vs. Temperature

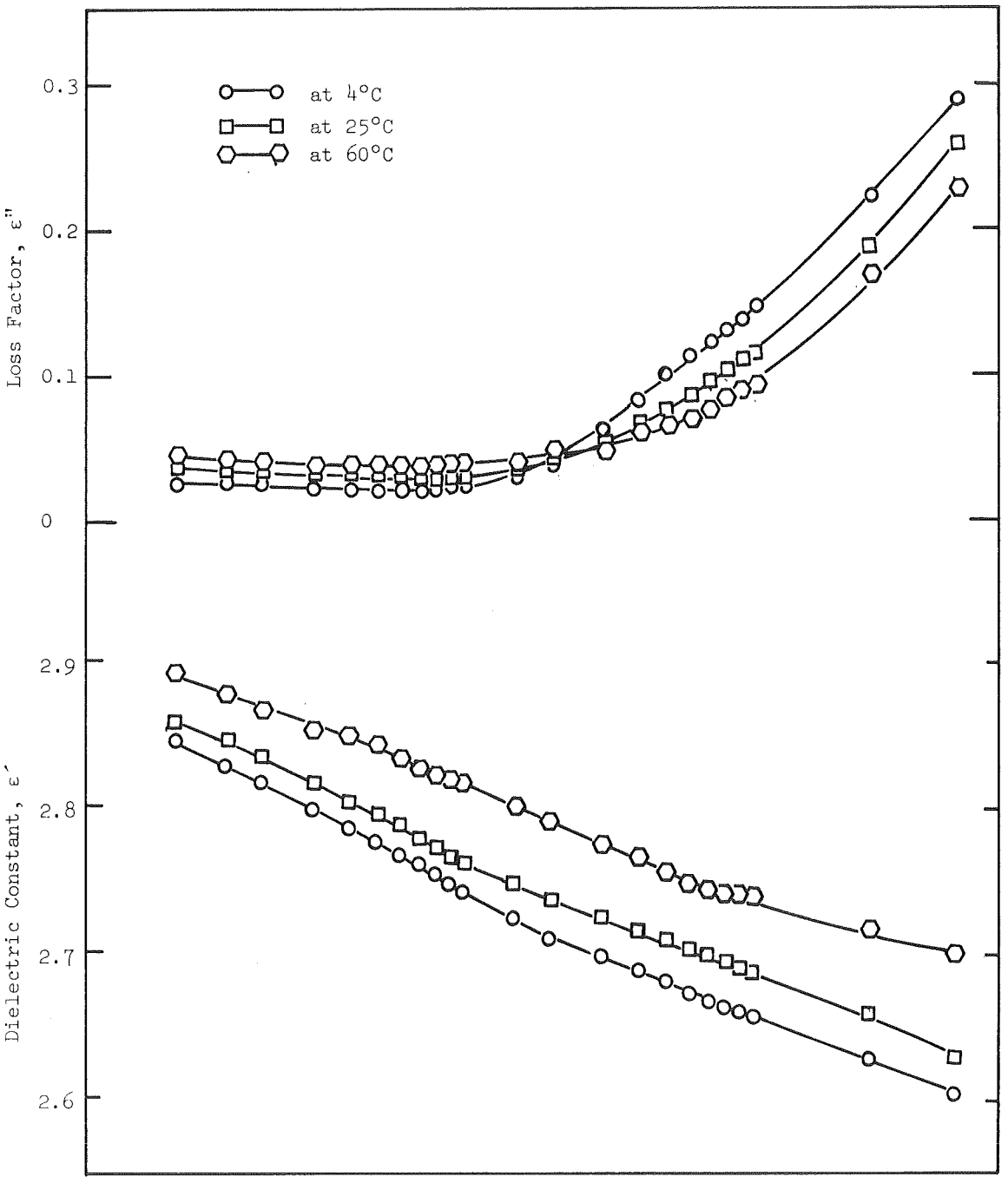

Fig - 19. Dielectric Constant vs. Frequency and Loss Factor vs. Frequency at Different Temperature, for Sample No. 48 133A

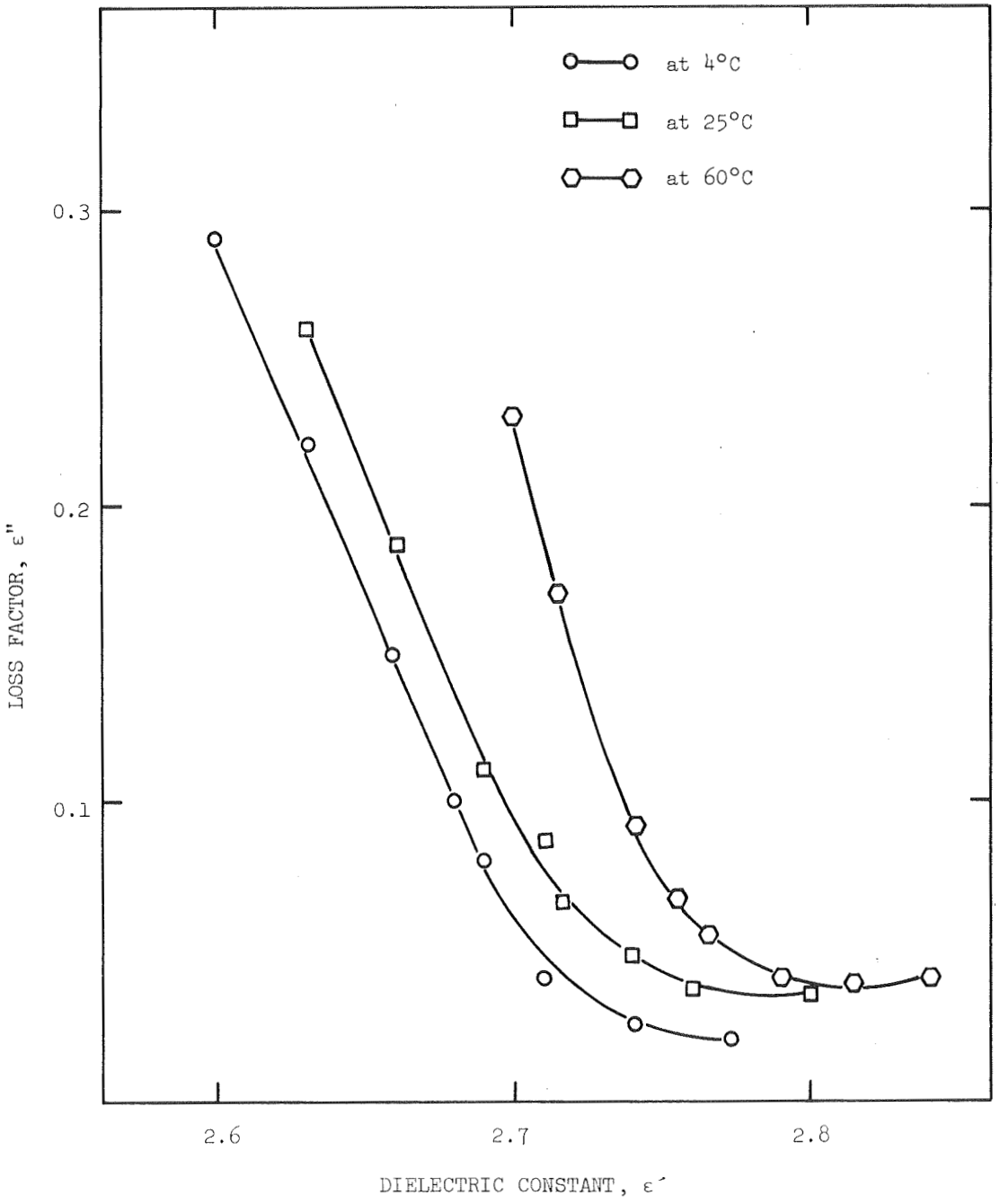

Fig -20. Loss Factor vs. Dielectric Constant at Different Temperature for Sample No. 48 133A

varies from sample to sample. As a general tendency, the capacitance changes more strongly with dc bias. For larger thickness at same dc bias field, thicker specimens have larger percentage change than thinner ones. The capacitance continues to increase nonlinearly with increasing dc bias voltage up to its breakdown. For a specimen of 128 Å thick, 6.5% increase in capacitance was observed at 2.8 V bias while it increased 2% at 1.4 V bias. Because of the inaccuracy in the measurement of the voltage across the specimen, the information is not precise.

D. D.C. Dielectric Strength

One of the most significant characteristic properties of thin films is that their thickness is very small compared to other dimensions. Frohlich[37] has shown the dielectric strength should increase as the thickness of a dielectric specimen decreases and approaches the length of the electron mean free path. Since avalanche and thermal breakdown are less likely to occur, intrinsic breakdown becomes the predominant mechanism in very thin films.

Four specimens with thickness from 80 to 420 Å have been tested by applying dc potential across two evaporated aluminum electrodes. The dielectric strength obtained fell within the range of 2 to 6 x 10^6 V/cm, but they showed no variation of dielectric strength with thickness within the range observed. It can be attributed to the amorphous nature of the polymer films as compared with ionic films, reducing the length of electron mean free path. The observed results are listed in Table 1.

Table I

Dielectric Strength of Polymerized DC-704 Films at 25°C

Sample No	Thickness Å	Capacitance p.f at 1 KHz	Dissipation Factor at 1 KHZ	DC Dielectric Strength V/cm
12	80	4050	0.0106	2.4×10^6
11	180	1803	0.0112	3.1×10^6
33	285	1285.4	0.0121	2.0×10^6
24	420	785.5	0.0116	6.0×10^6

Films formed by a higher energy (600 ev) electron beam showed a dielectric strength of less than 8×10^5 V/cm but no variation of dielectric strength with thickness is observed. The reduced dielectric strength may be regarded as the higher polymerization energy causing the films to be degraded into a more conductive state. Since the energy of the electron beam is many times more than that required to initiate the reaction[40], more bonds are broken than would be required to initiate the reaction. This inevitably results in a high concentration of free radicals and it is observed to have the effect of increasing the electron transport through the film.

E. Electrical Conductivity

As mentioned previously thin polymer films have the property to conduct appreciable non-ohmic currents as a function of thickness, surface contact, temperature and finally structural imperfections.

The general mechanism of current flow in insulators are electron tunneling, field emission, space-change-limited(SCL) conduction and impurity conduction. In the low temperature range for thinner films, the major contribution to current flow may be due to tunneling. The current decreases exponentially with increased thickness, and is usually negligibly small for thickness greater than about 100 Å. The emission of electrons by means of Richardson-Schottky mechanism is more significant, because a large electric field can induce a considerable current through the films. Schottky emission in polymerized silicone oil films with gold contacts has been observed[4]. The current density is quite sensitive to temperature. Space-change-limited current is possible for even thicker films and is very sensitive to the presence of trap sites in the films. Electrical conductivity is also possible in films which contain impurity centers which are capable of ionization. When an electric field is present the ions may move or electrons can "hop" from site to site in the film. This mode of conduction is referred to as Frenkel-Poole mechanism.

Figure 21 shows the plots of InI vs V for two specimens. The data was taken an hour after the specimens were moved from the vacuum chamber. A linear relationship between lnI and $V^{1/2}$ could be identified. It indicates that the conduction can be contributed to either Richardson-Schottky or space-change-limited current, probably the combination of tunneling, Schottky emission or field assisted emission from traps in the films can be attributed to the complex behavior. Some samples showed two distinct linear portions on a lnI vs $V^{1/2}$ which supports the conclusion that two or more mechanisms are present.

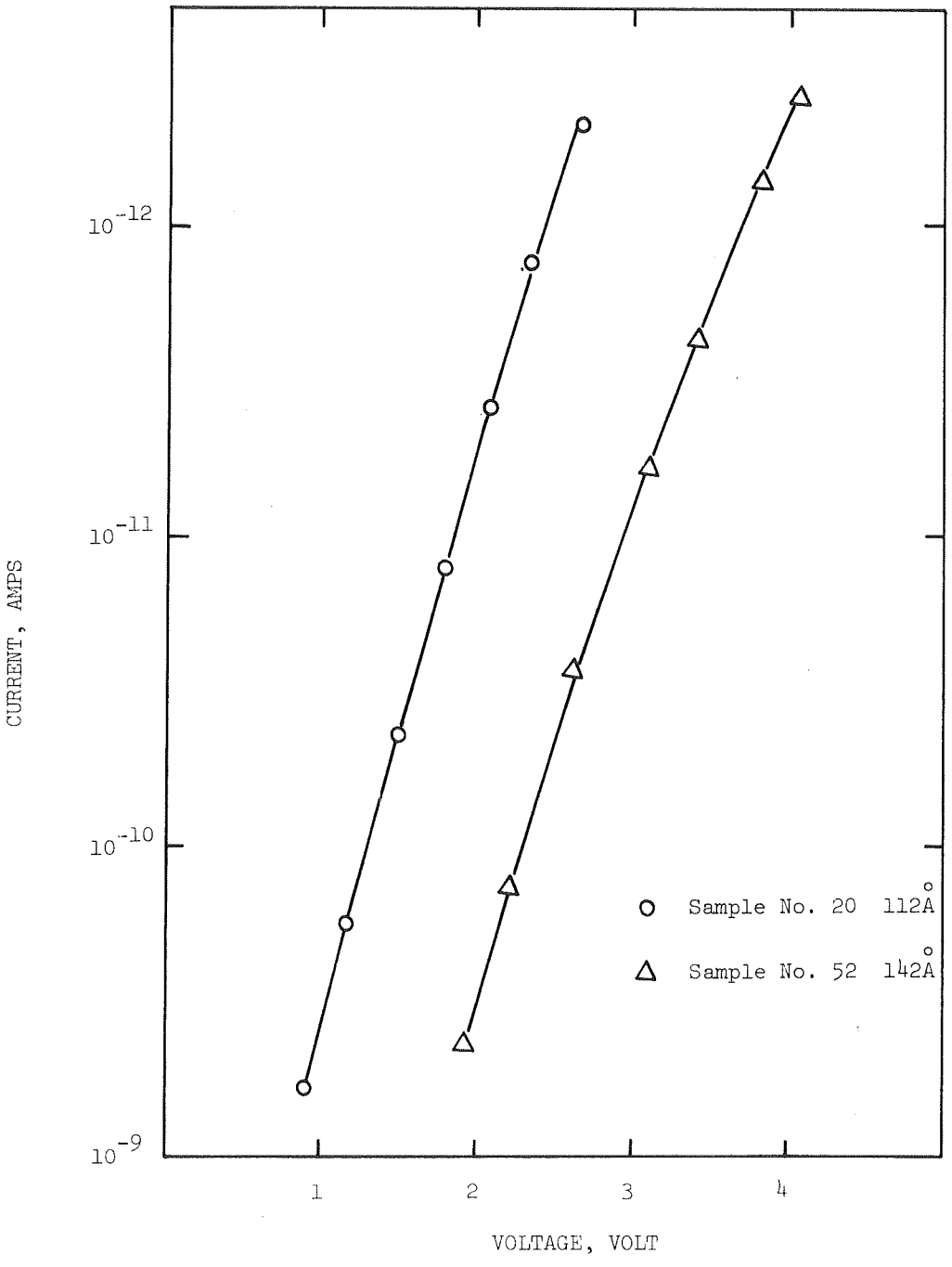

Fig - 21. V-I Characteristics

CHAPTER V

SUMMARY OF CONCLUSIONS AND RECOMMENDATIONS

A. Conclusions

Thin films of polymerized DC-704 oil can be formed by electron beam bombardment with reasonably good reliability and compatibility down to 50 Å. Detailed dielectric behavior of the films is strongly dependent on the method of formation and environmental conditions. Some specific conclusions can be drawn:

(1) The polymer films are homogenous in thickness and free from pinholes provided that the substrates are carefully prepared. The cross-linking of the polymer accounts for the toughness and durability of the films.

(2) The polymer film has two dielectric dispersions, a high frequency dispersion with a low frequency dispersion superimposed. It is likely that there are two or more mechanisms involved in the relaxation process. The relaxation time is estimated to be between 1.9 and 4.5×10^{-7} second for high frequency dispersion.

(3) The resultant percentage decrease in capacitance with time is a bulk function rather than a surface function. This is probably attributable to the absorption of oxygen instead of the absorption of moisture.

(4) The polymer film has a very high dielectric strength, routinely being higher than 10^6 volt/cm. This phenomenon is attributed to the increase of dielectric strength as the thickness of specimen decreases and approaches the length of the electron free path. Increase in the energy of formation results in a decrease of dielectric strength.

(5) The measured capacitance depends both on temperature and dc bias. The capacitance increases with increasing dc bias of temperature.

(6) Non-linear conductivity of the polymer film thicker then 100 Å could be described by several processes. It could have been various combination of mechanisms or it might be temperature dependent, a transition from one dominant mechanism to another taking place as the temperature varied.

B. Recommendations for Further Research

The investigations presented appear to indicate several interesting phenomena which probably warrant further study.

(1) Further theoretical research is needed to relate the investigated dielectric properties to molecular and inter-molecular structures.

(2) By extending the frequency range or making measurement at lower temperature, dielectric relaxation can be more completely observed.

(3) It is possible that the conduction through the polymer molecule is determined by its structure. The electrons have to overcome a potential barrier in going from one molecule to the next. The overall characteristic may be a function of the overlap of atomic orbitals within the polymer molecule and the overlap of molecular orbitals between polymer molecules. Thus, intramolecular conduction as well as intermolecular conduction should be investigated.

(4) To investigate the possible existance of bistable negative resistance phenomenon which has been observed for polymer films such as poly-divinlbenzene.

BIBLIOGRAPHY

1. A.E. Ennos, "The Sources of Electron-Induced Contamination in Kinetic Vacuum Systems", Brit. J. Appl. Phys. 5, 27 (1954)

2. K. M. Poole, "Electrode Contamination in Electron Optical Systems", Proc. Phys. Soc. (London) B.66, 452 (1953)

3. K. A. Buck and K. Shoulders,"An Approach to Microminimature Printed Circuits", Proc. Eastern Joint Computer Conf. Philadelphia, 55 (1958)

4. P. R. Emtage and W. Tantraporn, "Shottky Emission Through Thin Insulating Films", Phys. Rev. Letters 8, 267 (1962)

5. H. T. Mann, "Electrical Properties of Thin Polymer Films, Part I, Thickness 500-2500 Å" J. Appl. Phys. 35, 2173 (1964)

6. R. W. Christy, "Formation of Thin Polymer Film by Electron Bombardment", J. Appl. Phys. 31, 1680 (1960).

7. R. W. Christy, "Electrical Properties of Thin Polymer Films, Part II, Thickness 50-150 Å", J. Appl. Phys. 35, 2179 (1964)

8. G. W. Hill, "Electron Beam Polymerization of Insulating Films", Microelec. and Reliab, 4, 109 (1965).

9. L. Holland and L. Laurenson, "The Electrical Properties of Silicon Films Polymerized by Electron Bombardment", Vacuum, 14, 325 (1964).

10. D. S. Allam and C.T. H. Stoddart, "The Role of Organic Polymer in Thin Film Electronics", Chem Brit. 2, 410 (1965).

11. L. Holland and L. Laurenson, "The Secondary Electron Emission Characteristics of Clean and Contaminant Titanium", Suppl. Al. Nuovo Cimento, 1. 490 (1963).

12. G. W. Hill, "Deposition of Insulating Thin Films by Electron Beam Polymerization", Sym. Electron Beam Technique for Microelectronics, R.R.E. Malvern, July, 1964.

13. I. Haller and P. White, "Polymerization of Butadiene Gas in Surfaces under Low Energy Electron Bombardment", J. Phy. Chem, 67, 1784 (1963)

14. R. A. Fotland and W. J. Burkhard, Presented to Elect. Chem. Soc. Mtg, Los Angeles, May, 1962.

15. E. M. DaSilva and E. Klokholm, Elect. Chem. Soc. Mtg, Electric Insulation Div. Abstract No. 14, San Francisco, May, 1965.

16. A. E. Brennemann and L. V. Gregor, "Epoxy Dielectric Films Produced by Electron Bombardment", J. Elect. Chem. Soc., 112, 1194 (1965).

17. K. R. Shoulders, "Microelectronics Using Electron-Beam Activated Machining Techniques", Advances in Computers, 2, 135, (1965) Academic Press.

18. T. P. Woodman, "The Formation of Thin Films of Silica by the Electron Bombardment of Triphenylsiland" Brit. J. Appl. Phys. 16, 359 (1963)

19. Eugene T. Fitzgibbons , "Current Mechanism in Thin Polymer Films", Master Thesis, University of Texas, Austin, 1967.

20. J. G. Kirkwood and R. M. Fuoss, "Anomalous Dispersion and Dielectric Loss in Polar Polymer", J. Chem. Phys. 9, 329, (1964).

21. A. J. Curtis, "Dielectric Properties of Polymeric Systems ", Progress in Dielectrics Vol II, J. B. Birks, eds, John Wiley, New York, (1960).

22. W. G. Oakes and D. W. Robinson, "Dynamic Electrical and Mechanical Properties of Polythene Over a Wide Temperature Range", J. Polymer Sci. 14, 505, (1945).

23. Kenj Tage, "Mechanical and Dielectric Relaxation in Paraffin Crystal" Japanese J. Appl. Phys. 3, 588 (1964).

24. A. B. Lidiard, "Defects in Crystalline Solids", Phys Soc. Conf. Bristol, (1958), p. 283.

25. D. P Seraphin,"Electronic Properties of Thin Films", in "Thin Films", Am. Soc. Of Metals, 1963.

26. Debye, "Poler Molecules", Chemical Catalog Co. (1929).

27. C. Weaver, "Dielectric Properties of Evaporated Films" Adv. Phys. (London) 11, 83, (1962).

28. H. Frohlich, "Theory of Dielectrics", Oxford University Press (1949) Sec. 11.

29. J. C. Maxwell, "Electricity and Magnetism", 3rd ed, Oxford University Press, p. 452.

30. See J. B. Whitehead, "Lecture on Dielectric Theory and Insulation", McGraw Hill, New York, (1927) or C. P. Smyth, "Dielectric Behavior and Structure", McGraw-Hill, New York (1955), P. 73.

31. B. V. Harmon and R. J. Meakims, "Low-Frequency Dielectric Absorption in Organic Long-Chain Compound Due to the Presence of Traces of Alchol Impurities", Nature, 166, 29, (1950).

32. E. J. Murphy and S. O. Morgan, "The Dielectric Properties of Insulating Material, II, Alternating and Direct Current Conductivity", Bell. Sys. Tech. J. 18, 502, (1939)

33. W. C. Carter, "Dielectric Dispersion and Absorption in Natural Rubber Neoprene, Butaprene N M, and Butaprene S, Gum, and Treated Stocks", Trans. Faraday Soc. 42A, 206 (1946).

34. K. S. Cole and R. H. Cole, "Dispersion and Absorption in Dielectrics", J. Chem. Phys. 9, 341 (1941)

35. L. V. Gregor, "Polymer Dielectric Films", IBM J. Res and Dev. 12, 2, 140 (1968).

36. F. S. Maddock and R. E. Thun, "Properties of Evaporated Film Capacitors," J. Elect. Chem. Soc., 109, 99 (1962).

37. See. J. J. O'Dwyer, "Theory of Dielectric Breakdown in Solids," Clarendon Press, Oxford, (1964).

38. C. J. F. Bottcher, "Theory of Electric Polarization" Elsevier Pub. Co., Amsterdam, (1952) p. 346.

39. K. Okano, "Solid State Physics", Vol 14, Seitz. ed. Academic Press, Inc. (1963) p. 387.

40. P. White, "Preparation and Properties of Dielectric Layers Formed by Surface Irradiation Techniques"- Insulation 13, 5, 52, (1967).

41. P. White, "Thin Film Dielectrics," Insulation, 9, 9, 57 (1963).